[American Journal of Science, Vol. 321, April, 2021, P. 458–489, DOI 10.2475/04.2021.03]

SILURIAN-DEVONIAN TECTONIC EVOLUTION OF MID-COASTAL MAINE, U.S.A.: DETAILS OF POLYPHASE OROGENIC PROCESSES

DAVID P. WEST, JR.*,†, EMILY M. PETERMAN**, and JESSICA CHEN*

ABSTRACT. Detailed bedrock mapping, structural geology, meta-igneous whole rock geochemistry, and U-Pb geochronology from rocks sampled along a portion of a complexly deformed tectonic boundary between the Ordovician peri-Gondwanan Liberty-Orrington belt and Silurian syn-orogenic strata of the Fredericton trough (a.k.a. the Dog Bay Line) in mid-coastal Maine aid in deciphering the Silurian-Devonian tectonic evolution of the region. The new results provide constraints on several key events. First, initial terrane juxtapositioning occurred along the east-verging Boothbay thrust fault (D_1). This tectonism occurred prior to 423 Ma and is associated with the accretion of the Ganderian microcontinent to the Laurentian margin (that is, the Salinic orogeny). Subsequently, intrusion of an ultra-potassic magma, the protolith of the Edgecomb Gneiss, occurred at *ca.* 413 Ma. Its distinctive whole rock geochemical signature allows for correlation with rocks of similar composition and age along a relatively narrow 140 kilometer long distance on the northwestern margin of the Fredericton trough. This restricted area of ultra-potassic magma generation is attributed to the breakoff of the descending Salinic oceanic slab that triggered decompression melting of a previously metasomatized mantle wedge region beneath the accreted Ganderian microcontinent.

Early thrust faults (D_1) and the *ca.* 413 Edgecomb Gneiss igneous protolith were overprinted by an episode of upright folding (D_2) and low-pressure amphibolite facies metamorphism associated with the Early to Middle Devonian Acadian orogeny. Zircon overgrowths in the Edgecomb Gneiss dated at *ca.* 399 Ma grew during this tectonic episode. Comparisons with previous geochronological studies across the region suggest this dominant phase of Acadian deformation and metamorphism was long-lived (*ca.* 40 m.y.) and associated with the outboard accretion of the Avalonian microcontinent. Dextral shear structures represent the final phase of deformation (D_3) superimposed on this terrane boundary and are associated with the Norumbega fault and shear zone system that was active in Middle Devonian-Carboniferous time.

Key words: Appalachians, Salinic orogeny, Acadian orogeny, Ganderia, structural geology, tectonics, metamorphism, igneous geochemistry, U-Pb geochronology

INTRODUCTION

The hinterland portions of orogenic belts host complex zones of overprinting deformation, metamorphism and plutonism that have the effect of obscuring earlier relationships. These collective tectonic processes are the product of the piecemeal accretion of terranes and, in the case of the Appalachian orogenic belt, the accretion of multiple terranes onto the eastern margin of Laurentia during the Paleozoic. The initial arrival of individual terranes to the continental margin is but one phase of a long-lived multifaceted process of orogenic belt evolution. Unraveling the nature and timing of overprinting tectonism along terrane sutures provide a more holistic record of the thermal and deformational processes associated with polyphase terrane accretion.

The eastern margin of the northern Appalachians (fig. 1) preserves a number of different lithotectonic belts that initially formed outboard of Laurentia (that is, peri-Gondwanan) in late Neoproterozoic to Ordovician time (Hibbard and others, 2007;

* Department of Geology, Middlebury College, Middlebury, Vermont 05753
** Department of Earth and Oceanographic Science, Bowdoin College, Brunswick, Maine 04011
† Corresponding author: Phone: 802-443-3476; e-mail: dwest@middlebury.edu

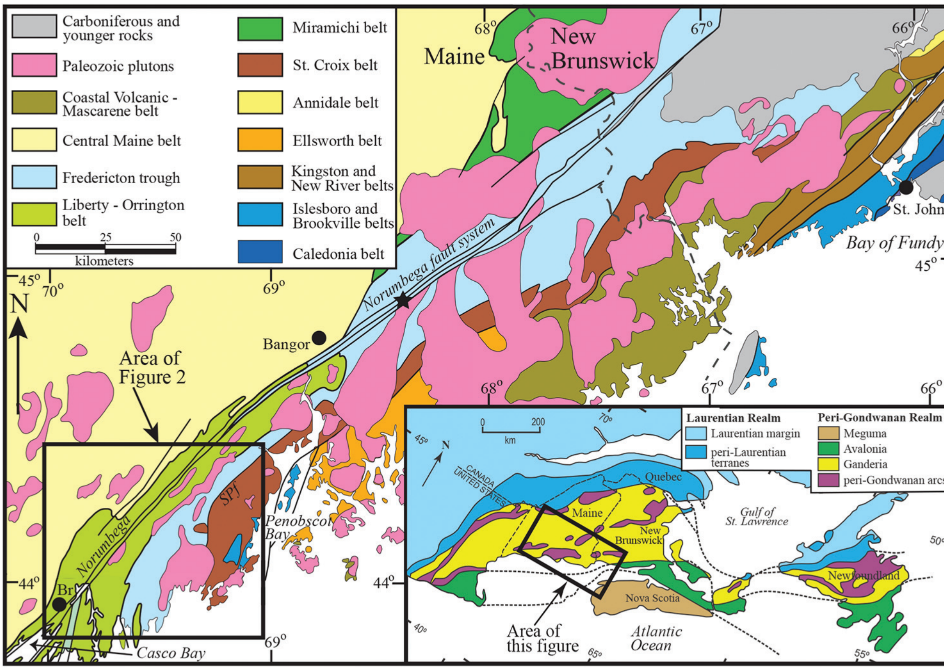

Fig. 1. Tectonic map of south-central and eastern Maine, and adjacent regions of coastal New Brunswick, modified from Hibbard and others (2006). The inset map, also modified from Hibbard and others (2006), shows this map location within the larger context of the northern Appalachians. The dark box in the lower left shows the area of greater detail provided in figure 2. The star marks the location of the small ultra-potassic Turner Mountain syenite referred to in the text (Wang and others, 2014). Br = Brunswick.

van Staal and Barr, 2012; Karabinos and others, 2017; Waldron and others, 2019). Subduction of intervening oceanic lithosphere resulted in the convergence and eventual progressive accretion of these outboard terranes, as well as the development of several syn-orogenic depositional basins that filled with thick sequences of Silurian strata (Bradley and others, 2000; Tremblay and Pinet, 2016). In mid-coastal Maine two of these regionally extensive terranes, metavolcanic and volcanogenic sedimentary rocks of the Ordovician peri-Gondwanan Liberty-Orrington belt and Silurian syn-orogenic metasedimentary strata of the Fredericton trough, are juxtaposed along a complex terrane boundary. This terrane boundary has been interpreted by Reusch and van Staal (2012) to represent a southern continuation of a major tectonic boundary in Newfoundland, the Dog Bay Line (Williams and others, 1993). Understanding the nature and evolution of this boundary is fundamental to unraveling the progressive nature of terrane accretionary processes in this region.

The purpose of this paper is to present a synthesis of detailed mapping, structural geology, meta-igneous whole rock geochemistry, and U-Pb geochronology to evaluate the timing of progressive deformation and metamorphism along the contact between Ordovician rocks of the Liberty-Orrington belt and Silurian strata of the Fredericton trough. An advantage of the study site is the presence of a deformed Early Devonian ultra-potassic intrusive rock, the Edgecomb Gneiss, that we propose is associated with a distinctive regional magmatic event. The occurrence of this plutonic rock along the tectonic boundary provides an important reference frame for the tectonic processes that both pre- and post-date the intrusion. Additionally, the unique geochemical signature of what herein is identified as a temporally and spatially restricted episode of

Early Devonian ultra-potassic magmatism places tight constraints on the tectonic setting during this time interval. Collectively, the multidisciplinary study of this important terrane boundary provides a near 50 million year record of progressive tectonic activity occurring in a key hinterland portion of the northern Appalachians.

REGIONAL GEOLOGIC SETTING

The study area is located in mid-coastal Maine, between Casco Bay to the southwest and Penobscot Bay to the northeast (figs. 1 and 2). The bedrock in this portion of the northern Appalachians is complex, having been deformed during multiple events, metamorphosed to amphibolite facies conditions, and intruded by several generations of plutons (Tucker and others, 2001; Gerbi and West, 2007) some of which were emplaced before and during deformation, thereby providing key constraints on the tectonic evolution of the region. A summary of both the stratified and plutonic rocks is provided below with a more detailed discussion of deformation and metamorphism presented in later sections titled Deformational History and Metamorphic History.

Lithotectonic Sequences

The stratified rocks in this region can be divided into numerous fault-bounded lithotectonic belts based on their ages and internal stratigraphy. Figures 1 and 2 present views of the regional spatial distribution of these belts at different scales, and figure 3 provides generalized stratigraphic columns showing the tectono-stratigraphic relationships between the different rock groups discussed in the paper. From west to east, the more extensive belts include (1) primarily Silurian metasedimentary rocks of the Central Maine sequence, (2) Ordovician metasedimentary and metavolcanic rocks of the Liberty-Orrington belt, (3) Silurian metasedimentary rocks of the Fredericton trough, and (4) a region underlain by several different peri-Gondwanan belts ranging in age from Late Precambrian to Ordovician. Two spatially restricted belts, the Late Ordovician to Early Silurian East Harpswell Group and the Cross River Formation of uncertain age, are shown in the Liberty-Orrington belt and Fredericton trough, respectively. A summary of the lithologies immediately proximal to the study area is provided below; the reader is referred to Berry and Osberg (1989), Tucker and others (2001), Hussey and Berry (2002), and Fyffe and others (2011) for the details of rock types present, constraints on protolith ages, and interpretations of the contact relationships between the different belts shown in figures 1 and 2.

The Ordovician Liberty-Orrington belt is exposed immediately southeast of the extensive, largely Silurian metasedimentary rocks of the Central Maine basin (fig. 2). The relatively narrow (< 25 kilometers) nearly 175-kilometer-long belt contains metamorphosed Middle to Late Ordovician volcanic and volcanogenic sedimentary rocks of the Falmouth-Brunswick Group and the Casco Bay Group (Hussey and others, 2010). These rocks are interpreted to represent an assemblage of volcanic arc to back-arc rocks of Gondwanan affinity (that is, Ganderia) that were accreted to the Laurentian margin during the Silurian (West and others, 2004; Hussey and others, 2010). Rocks of the Falmouth-Brunswick sequence and Casco Bay Group are juxtaposed along various faults and shear zones associated with the Norumbega fault system (Ludman and West, 1999). Within the study area (fig. 4), only the metasedimentary Cape Elizabeth Formation of the Casco Bay Group is present, with other formations (that is, Cushing, Spring Point, Diamond Island, and Scarboro formations) interpreted to be missing due to faulting (see below).

Included within the Liberty-Orrington belt in figures 1 and 2 is a thin belt of enigmatic rocks known as the Passagassawakeag Gneiss (shown in fig. 4). First defined by Bickel (1976), these rocks are now known to be continuous for nearly 75 kilometers

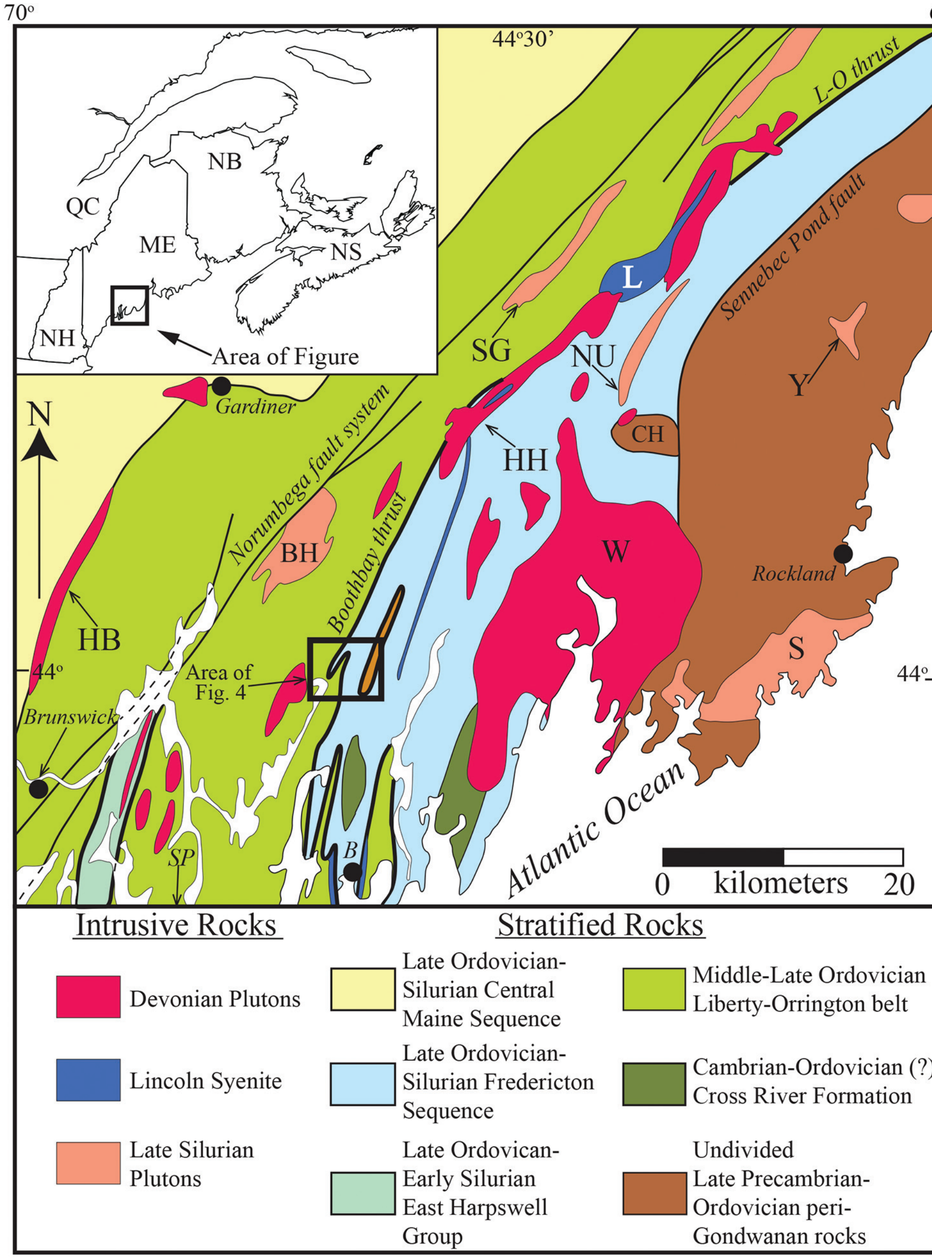

Fig. 2. Generalized geologic map of mid-coastal Maine showing the major lithotectonic belts, bounding faults, and Paleozoic intrusive rock bodies (modified from Osberg and others, 1985; Hussey and Marvinney, 2002; Gerbi and West, 2007). BH = Blinn Hill granite gneiss (424 ± 2 Ma); HB = Hornbeam Hill granite gneiss (393 ± 4 Ma: Gerbi and West, 2007); HH = Haskell Hill granite gneiss (408 ± 5 Ma); SG = Lake St. George granite gneiss (422 ± 2 Ma); L = Lincoln syenite (418 ± 1 Ma); L-O = Liberty-Orrington thrust; NU = North Union granite gneiss (422 ± 2 Ma); S = Spruce Head granite (421 ± 1 Ma); W = Waldoboro granite (368 ± 2 Ma); Y = Youngtown granite (420 ± 2 Ma), CH = Clarry Hill Formation (see Berry and others 2016 for a discussion of the emplacement of these rocks along the Clarry Hill thrust, which is in turn cut by the Sennebec Pond fault). *B* = Boothbay Harbor; *SP* = Small Point located ~10 kilometers south. Unless otherwise indicated, all quoted ages are U-Pb zircon ages from Tucker and others (2001). The black box outlines the area of figure 4.

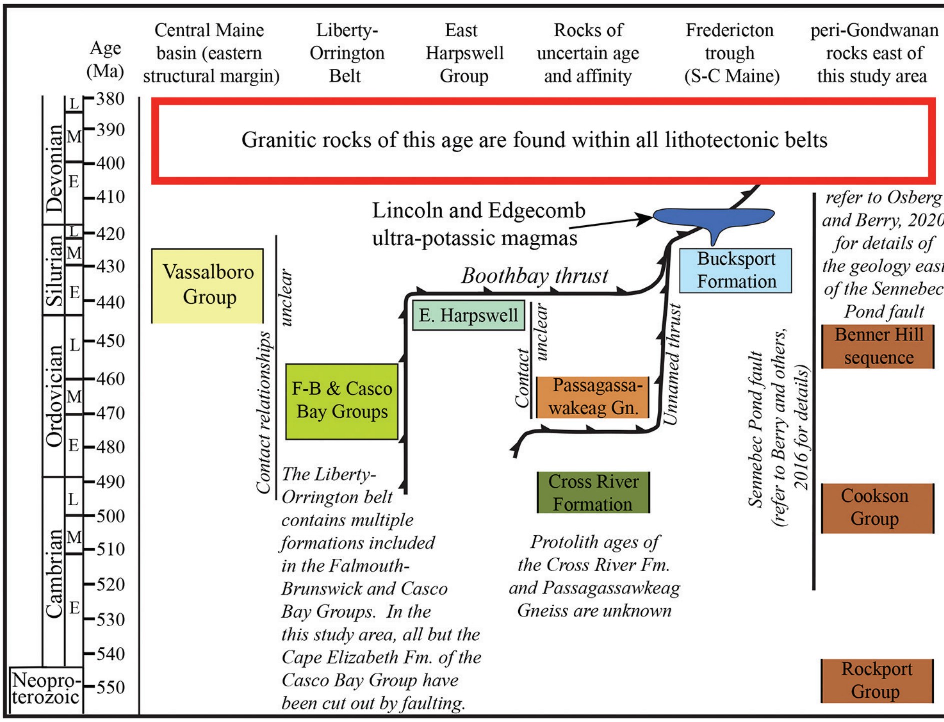

Fig. 3. Generalized stratigraphic columns showing the tectonostratigraphic relationships between the different rock groups discussed in the paper. Refer to Hussey and others (2010) and Cartwright and others (2019) for the details of individual units within all areas except the peri-Gondwanan rocks east of the study area. Refer to Berry and others (2016) and Osberg and Berry (2020) discussions of these rocks. Thrust faults between belts are schematically shown but their vertical positions on the diagram do not imply absolute ages of thrusting.

along the eastern margin of the Liberty-Orrington belt and represent a high-grade metamorphic complex that contains variable percentages of schist, sheared plutonic rocks, and migmatite (fig. 5E). Multiple phases of ductile deformation and high-grade metamorphism have hindered interpretations of the original protolith age and tectonic affinity of these rocks. Contact relationships between the Passagassawakeag Gneiss and its correlatives and adjacent stratified rock units are shown to be faulted in all areas where detailed mapping has been accomplished (for example, West, 2006; Grover, 2007; Pollock, 2018).

Southeast of the Casco Bay Group and Passagassawakeag Gneiss of the Liberty-Orrington belt lie metamorphosed Silurian turbidites of the Fredericton trough. This belt of rocks extends from southern New Brunswick (Kingsclear Group) southeastward through southern Maine and has been interpreted to represent sedimentation in a foredeep tectonic setting (van Staal and Williams, 1988; Fyffe and others, 2011; Dokken and others, 2018). The Merrimack trough in southern New England has been interpreted as a southern continuation of the Fredericton trough (Wintsch and others, 2007). In mid-coastal Maine, rocks of the Fredericton trough are represented by the Bucksport and Appleton Ridge formations, although only the Bucksport Formation is exposed in the study area.

Rocks included within the Ordovician Liberty-Orrington belt (for example, Casco Bay Group and Passagassawakeag Gneiss) and the younger Silurian rocks of the Fredericton trough are juxtaposed along the east-verging Boothbay thrust fault

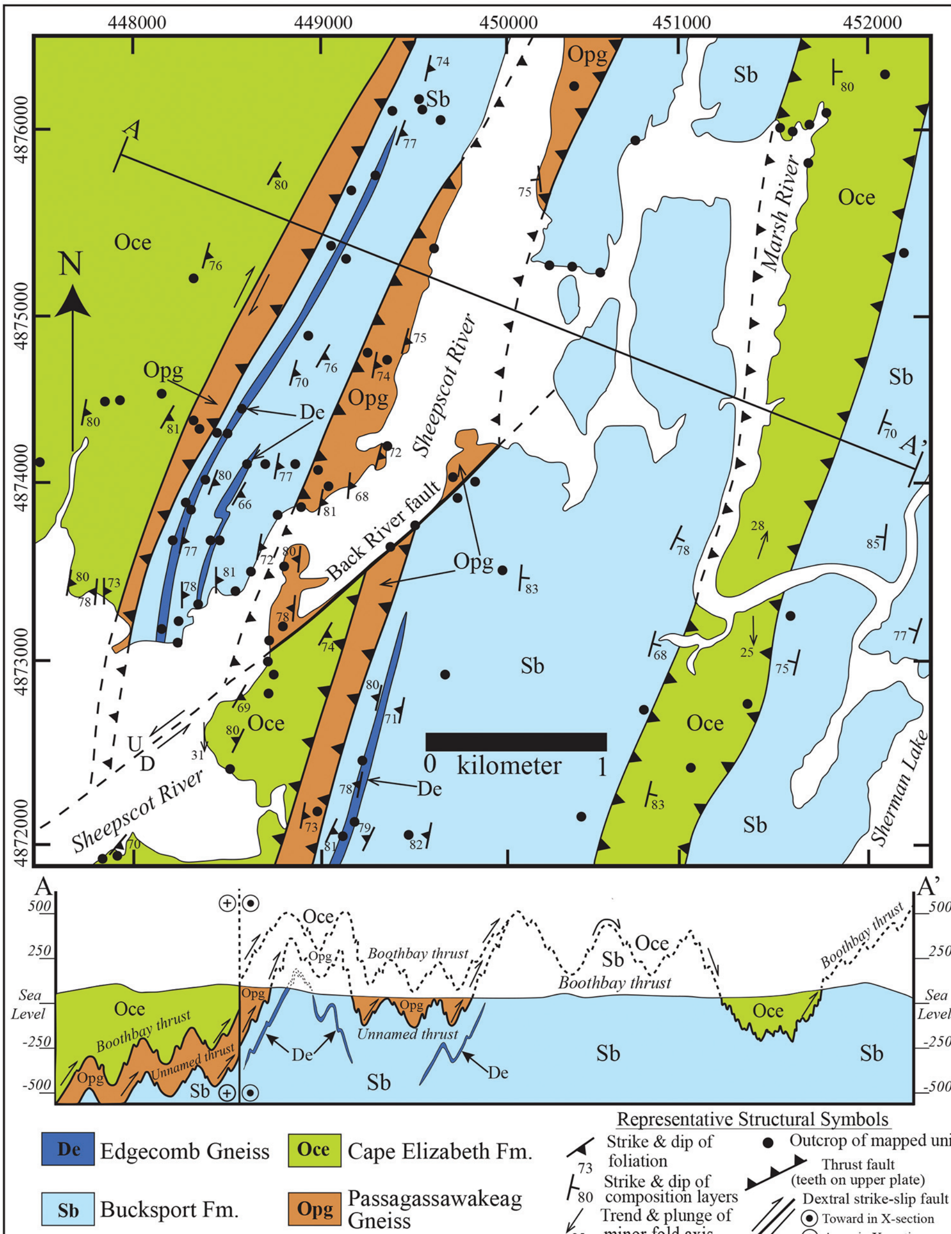

Fig. 4. Detailed geologic map of the study site and schematic cross section along A – A'. The reference lines along the margins of the map represent UTM 1000-meter grid lines (WGS 1984 data, Zone 19T). The map is modified from West (2016) and Grover and Newberg (2016) with areas to the east of grid line 450000 marking areas modified from Grover and Newberg (2016).

(Hussey, 1986; Hussey and Marvinney, 2002; Hussey and Berry, 2002). The Boothbay thrust, a subject of discussion below, likely correlates with the Liberty-Orrington thrust of Tucker and others (2001) in south-central Maine, and Reusch and van Staal (2012) correlate it with the Dog Bay Line in eastern Newfoundland (Williams and others,

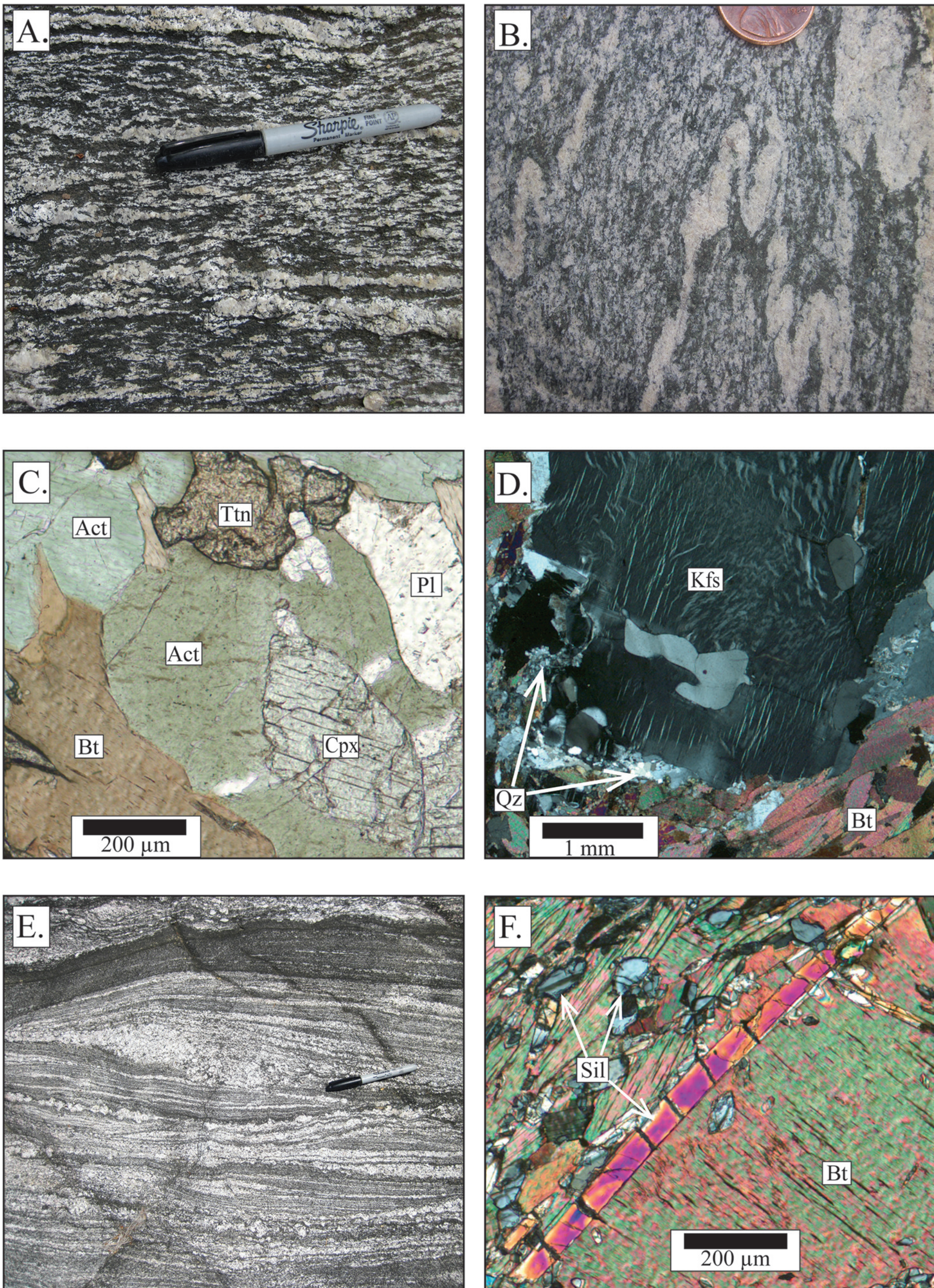

Fig. 5. Representative photographs from the study site. (A) Field photo of the Edgecomb Gneiss showing dark layers rich in clinopyroxene, actinolite and biotite, and lighter layers rich in K-feldspar, plagioclase, and quartz. (B) Cut slab showing the upright isoclinal folding of layering within the Edgecomb Gneiss. The folding of this gneissic layering is interpreted to reflect either the early stages of a progressive deformational path associated with D_2 folding, or the transposition of D_2 gneissic layering by superimposed D_3 dextral shear. (C) Plane light photomicrograph of the Edgecomb Gneiss showing metamorphic actinolite surrounding relict igneous clinopyroxene. (D) Plane light photomicrograph showing a relict igneous K-feldspar megacryst surrounded by recrystallized quartz. (E) Field photo of the Passagassawakeag Gneiss. (F) Crossed polarized light photomicrograph from a pelitic lithology in the Cape Elizabeth Formation showing prismatic sillimanite. Mineral abbreviations after Whitney and Evans (2010).

1993) and its southern extension into New Brunswick, the Bamford Brook fault (van Staal and others, 2009).

Plutonic Rocks

Several generations of intrusive igneous rocks are shown in figures 1 and 2, and as discussed below, their relationships to regional deformation and metamorphism provide critical constraints on the tectonic history of the region. The intrusive rocks shown in figure 2 can be divided into four general groups based on age, composition, and relationships to deformational fabrics in the surrounding stratified rocks.

(1) Late Silurian (420–425 Ma) granitoid rocks whose relationships to deformational events recorded in surrounding stratified rocks vary spatially across the region (fig. 2). East of the Sennebec Pond fault, Late Silurian intrusions (for example, Spruce Head and Youngtown plutons) are undeformed, whereas those to the west of this structure (for example, Blinn Hill, Lake St. George and North Union plutons) are strongly deformed.

(2) Late Silurian-Early Devonian (418 ± 1 Ma), variably deformed, ultra-potassic, Lincoln syenite. Extensive studies of the igneous petrogenesis (West and others, 2007), and overprinting deformation and metamorphism (Marsh and others, 2009) in the Lincoln syenite form a basis of comparison with the Edgecomb Gneiss in the present study area.

(3) Strongly foliated granitic rock bodies of Early to Middle Devonian age. The largest and most proximal of these is the Haskell Hill granite gneiss (408 ± 5 Ma: Tucker and others, 2001)

(4) Numerous non-foliated to weakly foliated, Middle to Late Devonian granites and granitic pegmatites distributed across the area of figure 2. The largest of these bodies includes the composite Waldoboro Complex (Barton and Sidle, 1994), a portion of which has an intrusive age of 368 ± 2 Ma (Tucker and others, 2001). Many of the mappable bodies and the smaller granites and pegmatites contain accessory muscovite and/or garnet characteristic of peraluminous compositions.

ANALYTICAL TECHNIQUES

U-Pb Geochronology

Zircon was separated at Middlebury College from Edgecomb Gneiss sample EG-17a using standard crushing, sieving, and magnetic and heavy liquid separation procedures. Separated grains were mounted in epoxy and the 1" (2.54 cm) diameter mount was progressively polished to expose the grain interiors. The mount was coated with < 10 nm of carbon to minimize charging during imaging. Zircon grains were imaged using the Tescan VEGA3 scanning electron microscope (SEM) at Bowdoin College via secondary electron (SE), backscattered electron (BSE), and cathodoluminescence (CL). BSE images were acquired using a 15 kV, 1 nA beam, with a working distance of 15 to 16 mm. SE and CL images were acquired with a 10 kV, ~300 pA beam at a working distance of 16 mm and scan speed of 0.03 to 0.1 ms/pxl. For CL imaging, brightness and gain were optimized at the start of the analytical session using black balancing techniques outlined in Peterman and others (2021); the same parameters were used for all images. Representative CL images of analyzed zircons are shown in the Appendix and figure 6.

Isotopic measurements were undertaken using the SHRIMP-RG, jointly operated by Stanford University and the USGS. The epoxy mount was polished with 1 μm diamond paste to remove the carbon coat, rinsed in 1M HCl, and dried in a vacuum

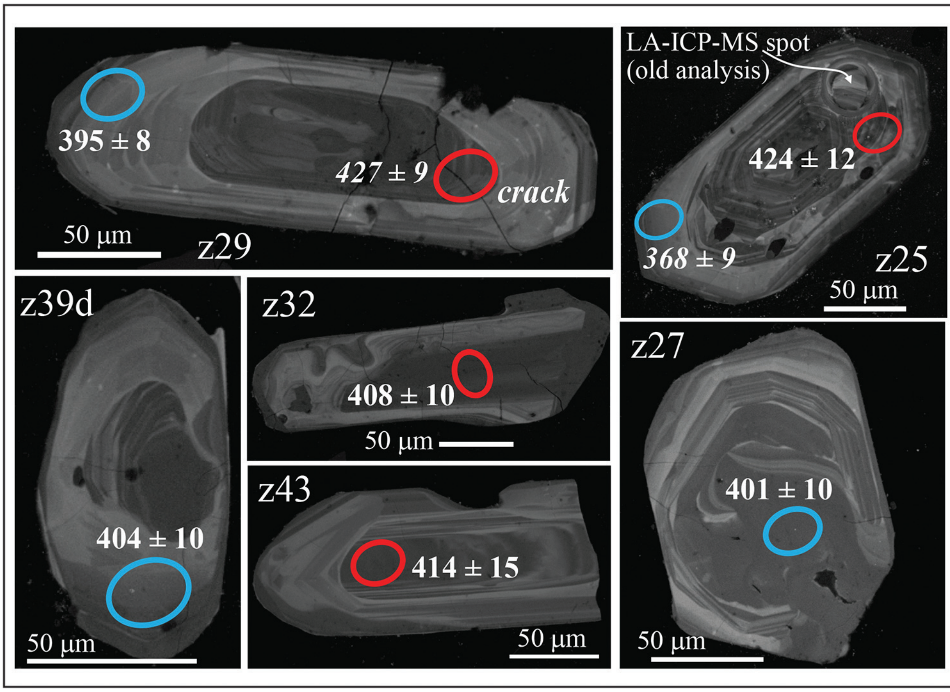

Fig. 6. Representative cathodoluminescence images of selected zircons analyzed from the Edgecomb Gneiss. The colors correspond to the different age domains shown in figure 7. Uncertainties on individual analyses are reported at 1σ.

sealed oven for 15 minutes prior to coating both sides with ~10 nm of Au. Secondary ions were generated using an O_2^- primary ion beam of 5 to 6 nA and a 100 μm aperture, which yielded a < 25 μm spot size. At the start of each acquisition, the sample surface was cleaned by rastering the primary beam for 60 seconds. Both the primary and secondary beams were auto-tuned to maximize transmission. The instrument was optimized for a mass resolving power of 8400 on ZrO, which was measured as an internal standard. For each measurement, five scans were completed through the mass table, which includes Zr_2O, ^{204}Pb, background, ^{206}Pb, ^{207}Pb, ^{208}Pb, ^{238}U, ThO, and UO. Isotopic ratios were corrected for common-Pb using ^{207}Pb, which assumes concordance. To evaluate the validity of this assumption, data were also corrected for common-Pb using ^{204}Pb and ^{208}Pb; the dates were equivalent within uncertainty using either correction. However, because ^{204}Pb and ^{208}Pb were analyzed for shorter intervals, we selected the ^{207}Pb-correction to correct the data for common-Pb. Temora (Black and others, 2003) was used as the age standard (418.37 ± 0.14 Ma; Mattinson, 2010); MAD-559 (Coble and others, 2018) was used as a concentration standard. Both standards were measured repeatedly during the analytical session. Data were processed following Coble and others (2018), which uses the MS Excel add-ins Squid 2.51 (Ludwig, 2009) and Isoplot 4 (Ludwig, 2012).

Major and Trace Element Geochemistry

Ten samples representing a range of bulk rock compositions identified through field and petrographic observations were selected for whole-rock geochemical analysis. These samples were crushed in a porcelain jaw crusher and powdered in an alumina ceramic shatterbox. Major element analysis of the samples, along with two standards, were completed using standard X-ray fluorescence techniques at Middlebury College (Thermo Scientific ARL Quant'x EDXRF Analyzer). Trace element analyses were completed at Middlebury College using a Thermo Scientific iCAP Q ICP-MS. Dilutions of 1000x for Rare Earth Elements and 2000x for other trace elements were made to bring the element counts into the optimal detection range for the instrument. Internal standards were also added to each dilution, and standardized reference solutions were also checked to monitor performance.

RESULTS OF DETAILED GEOLOGIC MAPPING

The study area (fig. 4), just northeast of the village of Wiscasset, straddles the contact between the Liberty-Orrington belt and the Fredericton trough, two regionally extensive terranes in the northern Appalachians. As with most terrane boundaries in the hinterlands of orogenic belts, this one has been modified by polyphase deformation and high-grade metamorphism. However, the presence of a strongly deformed intrusive rock body - the Edgecomb Gneiss - provides an opportunity to unravel the polyphase tectonic history of this boundary. This deformed intrusion is noteworthy in that: (1) its distinctive ultra-potassic composition can be linked to other intrusions of similar age along strike that share a comparable geochemical fingerprint (for example, the Lincoln syenite; West and others, 2007; the Turner Mountain syenite; Wang and others, 2014, see fig. 1 for locations), thus providing valuable constraints on the tectonic setting and processes responsible for the unique magma generation. (2) Because the timing of igneous crystallization can be determined, its relationship to deformational and metamorphic events provides important temporal constraints on the deformation and metamorphism along the terrane boundary.

Relationships Among Mapped Units

The geological relationships portrayed in figure 4 are based on recently published 1:24,000 scale mapping of the Wiscasset (West, 2016) and Damariscotta (Grover and Newberg, 2016) 7.5' quadrangles. The four rock main rock units in the study area are distinctive and easily distinguished from one another in the field.

Ordovician metasedimentary rocks of the Cape Elizabeth Formation of the Casco Bay Group are quartz-plagioclase-muscovite-biotite ± garnet ± sillimanite schists interlayered with quartz-plagioclase-micaceous granofels. For clarity, a thin and discontinuous porphyroclastic pelitic schist sub-unit of the Cape Elizabeth Formation, mapped separately by West (2016), is not shown in figure 4. The depositional age of the Cape Elizabeth Formation is tightly constrained between a 465 ± 4 Ma zircon from a volcanic rock in the underlying Cushing Formation (Hussey and others, 2010) and a 469 ± 3 Ma zircon from a volcanic rock in the overlying Spring Point Formation (Tucker and others, 2001). Importantly, neither the conformably underlying rocks of the Cushing Formation, nor the conformably overlying rocks of the Spring Point Formation (Hussey and others, 2010) are present in the study area and thus we interpret contacts of the Cape Elizabeth Formation with all other stratified rock units in the area to be fault contacts.

The Passagassawakeag Gneiss in the study area is dominated by porphyroclastic, quartz-plagioclase-biotite-K-feldspar gneiss (see fig. 5E) and minor amounts of mylonitic, porphyroclastic, sillimanite-bearing mica schist. Protolith ages of these rocks are unknown and contact relationships with adjacent stratified rock units have consistently been interpreted as tectonic along the length of the belt (for example, West, 2006; Grover, 2007; Pollock, 2018). We suggest here that the Passagassawakeag Gneiss represents an imbricate fault slice associated with the Boothbay thrust. This interpretation is consistent with findings along the length of the eastern margin of the Liberty-Orrington belt where it is in contact with rocks of the Fredericton trough.

Specifically, the Passagassawakeag Gneiss is variably present along the Boothbay thrust contact between the two lithotectonic belts. This relationship is well illustrated in the field area (fig. 4) where the gneiss unit is found between rocks of the Fredericton trough (Bucksport Fm.) and Casco Bay Group (Cape Elizabeth Fm.) in the western part of the field area, but is not present at this same contact on the east side of the map area. Thus, in the figure 4 cross-section, we show a progressive thinning and eventual termination of the thrust fault bounded Passagassawakeag Gneiss to the east. It is not clear from our work whether this occurred during D_1 thrusting, whether it is a consequence of superimposed D_2 and D_3 events, or both.

Rocks of the Silurian Bucksport Formation in mid-coastal Maine are quartz-plagioclase-biotite granofels interlayered with plagioclase-quartz-actinolite-diopside granofels. This monotonous sequence of interlayered biotite and calc-silicate granofels are interpreted to represent metamorphosed turbidite deposits. These rocks, previously mapped as the Sebascodegan Formation by Hussey (1992), have been correlated with the Flume Ridge Formation in eastern Maine and southern New Brunswick (Ludman and others, 2018) and thus represent the southern-most extension of the Fredericton trough. The depositional age of the Bucksport Formation in Maine is not constrained by fossils or radiometric ages, but rather is based on correlations with rocks of the Kingsclear Group in southern New Brunswick (McKerrow and Ziegler, 1971; Fyffe and others 2011; Dokken and others, 2018).

EDGECOMB GNEISS DESCRIPTION, GEOCHRONOLOGY AND GEOCHEMISTRY

The Edgecomb Gneiss, first recognized by Hatheway (ms, 1969), is a medium to dark gray, plagioclase-K-feldspar-biotite-quartz-hornblende ± clinopyroxene gneiss. The rock is characterized by large, light-colored, K-feldspar and plagioclase augen set in a finer-grained matrix of quartz, plagioclase, biotite, and hornblende (fig. 5A). The mineralogy, texture, and whole rock geochemical signatures (discussed below) indicate the Edgecomb Gneiss represents a deformed and metamorphosed intrusive rock of intermediate composition. In the study area (fig. 4), the rocks are found as thin sills (< 50 meters across) within the Bucksport Formation near its western margin. Importantly, these rocks are deformed by upright folds (fig. 5B) and associated steeply dipping penetrative foliation.

U-Pb Geochronology

Thirty-seven U-Pb dates calculated from zircon grains separated from a single sample of Edgecomb Gneiss (EG-17a) are presented in table 1 and shown graphically in figure 7. Of these 37 analyses, 11 were >18% discordant and thus not included in age calculations, and 3 were located along cracks and discarded. CL images with spot locations and U-Pb dates of all grains are provided in the Appendix. Several grains contain two domains that are distinguished by texture, age, and CL intensity. Many grains contain a xenocrystic core that exhibits oscillatory zoning consistent with a magmatic origin. Dates from these domains range from ~444 Ma to >1.62 Ga (table 1).

One population of zircon grains yield a mean age of 412.6 ± 6.0 Ma (2σ, n = 11; MSWD = 0.52). These dates were mostly measured from the cores of zircon grains (fig. 6 and Appendix) and, in rare cases, from domains that mantle xenocrystic cores and are also surrounded by a thin rim (for example, z41; Appendix). Zircon domains from this age population typically exhibit oscillatory or sector zoning.

A second population of zircon grains yield a mean age of 399.3 ± 6.6 Ma (2σ, n = 8; MSWD = 0.59). The majority of dates measured from this population are found as rims mantling older cores. A few spots were measured from domains that are located in the physical core of the grain, but cross-cutting relationships of these “invader”

TABLE 1

U-Pb isotopic data for zircons from Edgecomb Gneiss Sample EG-17a (UTM Location: 448483E, 4873779N, Zone 19N)

Spot Name	Type	U (ppm)	Th (ppm)	Th/U	Calculated Ages: $^{206}Pb^{\wedge}/^{238}U$ Age (Ma)	1σ (Ma)	$^{206}Pb†/^{238}U$	1σ (Ma)	$^{207}Pb†/^{206}Pb$ Age (Ma)	1σ (Ma)	% Discordance	Inverse Concordia Data: $^{238}U†/^{206}Pb^*$	1σ (Ma)	$^{207}Pb^*†/^{206}Pb^*$	1σ (Ma)	Conventional Concordia Data: $^{207}Pb^*†/^{235}U$	1σ (Ma)	$^{206}Pb^*†/^{238}U$	1σ (Ma)	err corr
EG-Z01	R	114	108	0.98	386	10	386	10	353	61	-9	16.22	2.7	0.0536	2.7	0.455	3.8	0.0616	2.7	0.7
EG-Z05	C	161	91	0.58	411	10	410	10	354	51	-17	15.21	2.5	0.0536	2.3	0.486	3.4	0.0657	2.5	0.7
EG-Z06a	R #	681	286	0.43	375	8	375	8	364	22	-3	16.69	2.1	0.0538	1.0	0.445	2.3	0.0599	2.1	0.9
EG-Z07a	C	94	73	0.80	417	13	417	12	400	70	-4	14.96	3.1	0.0547	3.1	0.504	4.4	0.0668	3.1	0.7
EG-Z07b	R	725	396	0.56	410	10	410	10	384	21	-7	15.24	2.6	0.0543	0.9	0.491	2.7	0.0656	2.6	0.9
EG-Z07c		185	156	0.87	384	8	386	8	514	82	+26	16.21	2.2	0.0576	3.7	0.490	4.3	0.0617	2.2	0.5
EG-Z10		207	153	0.76	433	12	431	12	307	45	-42	14.45	2.9	0.0525	2.0	0.501	3.5	0.0692	2.9	0.8
EG-Z12	C	351	239	0.70	406	10	406	10	370	34	-10	15.39	2.5	0.0540	1.5	0.484	2.9	0.0650	2.5	0.9
EG-Z13		361	363	1.04	410	7	409	7	342	31	-20	15.26	1.8	0.0533	1.4	0.482	2.3	0.0655	1.8	0.8
EG-Z18a		151	129	0.88	450	13	448	13	266	57	-71	13.90	2.9	0.0516	2.5	0.512	3.8	0.0720	2.9	0.8
EG-Z18b	X	366	197	0.56	444	10	444	9	413	26	-8	14.04	2.2	0.0550	1.2	0.540	2.5	0.0712	2.2	0.9
EG-Z23		140	83	0.61	424	11	441	10	1403	394	+71	14.11	2.2	0.0890	20.6	0.869	20.7	0.0709	2.2	0.1
EG-Z25	C	547	437	0.82	424	12	424	12	389	23	-9	14.71	2.9	0.0544	1.0	0.510	3.0	0.0680	2.9	0.9
EG-Z25b		360	135	0.39	368	9	367	9	309	34	-19	17.07	2.4	0.0525	1.5	0.424	2.8	0.0586	2.4	0.8
EG-Z27	R	606	138	0.24	401	10	401	10	401	24	+0	15.59	2.5	0.0547	1.1	0.484	2.7	0.0641	2.5	0.9
EG-Z28a		336	154	0.48	1292	40	1316	38	1624	11	+21	4.41	3.2	0.1000	0.6	3.123	3.2	0.2266	3.2	1.0
EG-Z28b	X	225	116	0.53	1613	40	1617	36	1652	12	+2	3.51	2.5	0.1015	0.6	3.990	2.6	0.2851	2.5	1.0
EG-Z29a	R	653	459	0.73	395	8	396	7	459	22	+14	15.80	1.9	0.0562	1.0	0.490	2.2	0.0633	1.9	0.9
EG-Z29b	C #	166	144	0.90	427	9	426	9	367	46	-17	14.64	2.1	0.0539	2.0	0.508	2.9	0.0683	2.1	0.7
EG-Z32	C	1380	1271	0.95	408	10	407	10	389	14	-5	15.33	2.5	0.0544	0.6	0.489	2.6	0.0652	2.5	1.0
EG-Z35a		372	125	0.35	473	21	475	21	607	74	+23	13.09	4.5	0.0601	3.4		5.7	0.0764	4.5	0.8
EG-Z35b	X	486	84	0.18	1194	34	1205	32	1382	30	+14	4.87	2.9	0.0880	1.5	2.493	3.3	0.2055	2.9	0.9
EG-Z36	C	128	98	0.79	408	9	408	8	376	50	-9	15.31	2.1	0.0541	2.2	0.487	3.1	0.0653	2.1	0.7
EG-Z39a		1710	94	0.06	374	7	376	7	507	293	+27	16.67	1.8	0.0574	13.3	0.475	13.5	0.0600	1.8	0.1
EG-Z39B		119	76	0.66	417	12	415	12	275	106	-53	15.02	3.0	0.0518	4.6	0.475	5.5	0.0666	3.0	0.5
EG-Z39c	C #	123	77	0.64	418	13	418	13	421	55	+1	14.94	3.2	0.0552	2.5	0.510	4.0	0.0669	3.2	0.8
EG-Z39d	R	476	0	0.97	404	10	404	9	433	25	+7	15.46	2.4	0.0555	1.1	0.495	2.6	0.0647	2.4	0.9
EG-Z40a	C	817	244	0.31	410	9	409	9	385	21	-7	15.26	2.3	0.0543	0.9	0.491	2.5	0.0655	2.3	0.9
EG-Z40b		222	109	0.51	398	11	397	10	312	98	-28	15.76	2.7	0.0526	4.3	0.460	5.1	0.0634	2.7	0.5
EG-Z41a	C	235	175	0.77	416	8	416	8	448	36	+7	14.98	2.0	0.0559	1.6	0.514	2.5	0.0667	2.0	0.8
EG-Z41b		163	101	0.64	421	14	419	14	336	55	-26	14.87	3.4	0.0532	2.4	0.493	4.2	0.0672	3.4	0.8
EG-Z41c	R	217	223	1.06	400	7	400	7	377	70	-6	15.64	1.8	0.0542	3.1	0.477	3.6	0.0639	1.8	0.5
EG-Z41d	R	622	123	0.20	411	14	411	14	379	22	-9	15.20	3.6	0.0542	1.0	0.492	3.7	0.0658	3.6	1.0
EG-Z45	C	260	130	0.52	425	9	425	9	439	44	+3	14.67	2.2	0.0557	2.0	0.523	3.0	0.0682	2.2	0.8
EG-Z47a	R	1715	94	0.06	395	13	395	13	394	12	-0	15.83	3.5	0.0546	0.6	0.475	3.5	0.0632	3.5	1.0
EG-Z47b	C	556	766	1.42	400	12	401	12	430	35	+7	15.60	3.0	0.0554	1.6	0.490	3.4	0.0641	3.0	0.9
EG-Z48	C	513	549	1.11	414	15	414	15	444	24	+7	15.06	3.7	0.0558	1.1	0.511	3.9	0.0664	3.7	1.0

C = igneous crystallization
X = xenocryst
R = rim; later growth
italic = discordant; not used in age calculations

†corrected for common Pb using ^{204}Pb
^corrected for common Pb using ^{207}Pb
* radiogenic Pb
# analysis hit a crack; discarded

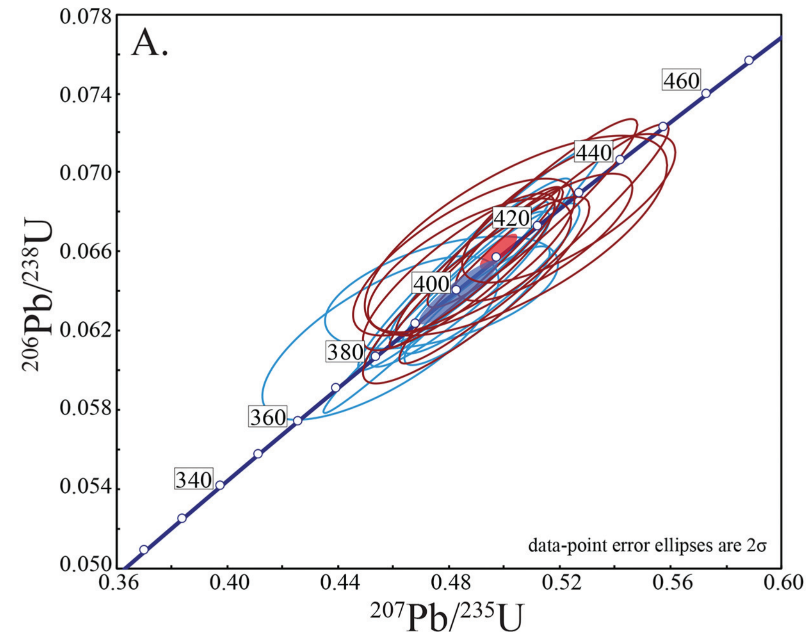

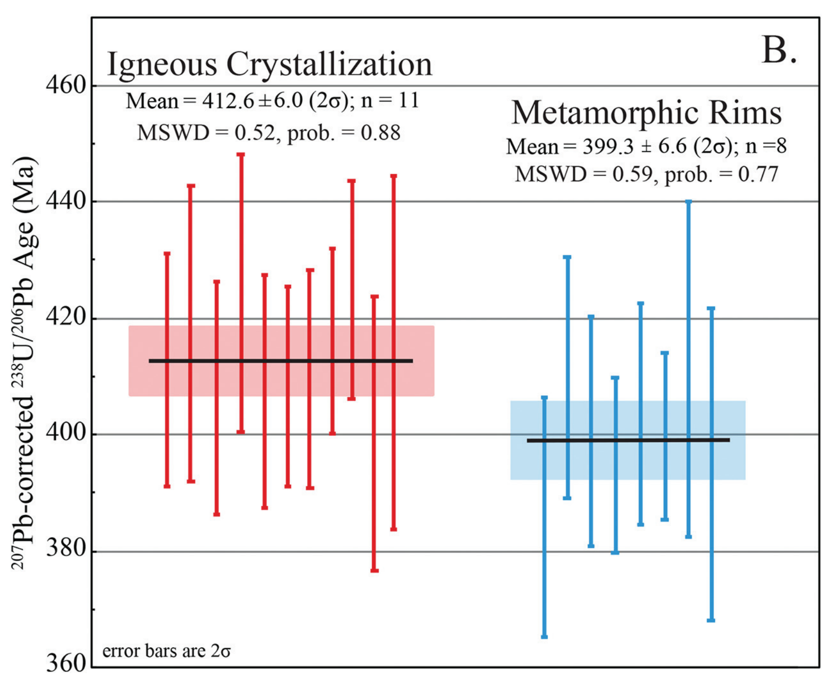

Fig. 7. U-Pb results from zircons analyzed from the Edgecomb Gneiss. (A) Concordia diagram covering the range of ages for concordant zircon analyses from sample EG-17a. The different color ellipses correspond to the different age domains shown in B; shaded ellipses represent the Concordant Age calculated for each domain. (B) ^{207}Pb corrected ^{238}U/^{206}Pb ages from the different zircon age domains. Data from all of the individual analyses are provided in table 1.

rims (fig. 6, z27) are consistent with an origin as a younger rim. Although some analyses yielded concordant, younger dates, these spots hit a crack and were thus not included in the calculated mean age for this domain.

Major and Trace Element Geochemistry

The whole rock major and trace element compositions of ten representative samples of the Edgecomb Gneiss are presented in table 2. Major element Harker diagrams (fig. 8) show the rocks to be intermediate in terms of their SiO_2 concentrations (56–62 wt.%) and notably elevated in K_2O (3.4–5.8 wt.%) and MgO (5.4–8.1 wt.%) concentrations. All but one of the samples analyzed meet the definition for ultra-potassic rocks as defined by Foley and others (1987), in that they have MgO $> 3\%$, $K_2O > 3\%$, and $K_2O/Na_2O > 2.0$. In terms of trace elements (fig. 9), the rocks are generally characterized by relatively high concentrations of Ba, (1107–1883 ppm), Sr (369–579 ppm), Ni (104–434 ppm), and Cr (264–433).

A plot of chondrite-normalized rare earth elements (REE) reveals a tight clustering of data and similar patterns for all samples analyzed (fig. 10A). The rocks are significantly more enriched in the light REEs (200 to 350 times chondritic abundances) relative to heavy REEs (only 10 to 20 times chondritic abundances). A slight negative Eu anomaly occurs in all samples. A primitive mantle-normalized extended trace element diagram (fig. 10B) shows that all the Edgecomb Gneiss samples are strongly enriched in incompatible elements (plotted on the left side of the diagram) relative to less incompatible elements (right side). A distinct negative anomaly is seen for Nb (relative to U and K), with less pronounced negative anomalies for Sr (relative to Pr and P), and Ti (relative to Eu and Dy).

DEFORMATIONAL HISTORY

Our observations in the study area are consistent with previous studies in the region (Hussey and Berry, 2002; Eusden and others, 2016) and suggest at least four distinct phases of deformation. The relative age relationships between these different events are described below and the absolute age constraints are provided by U-Pb zircon dates presented in this study and elsewhere.

Early thrust faulting (D_1 deformation).—The earliest documented phase of deformation in the region involves the thrusting of the Casco Bay Group over the Fredericton trough along the east-verging Boothbay thrust fault (Hussey and Berry, 2002). Rare, small-scale recumbent folds proximal to the field area (for example, Stop 3b of West and Condit, 2016) may be associated with this phase of deformation and have been documented elsewhere in the region (for example, Small Point area, see Hussey, 1988 fig. 6A, and Eusden and others, 2016; and Boothbay area, see Hussey and Berry, 2002, their fig. 45). It should be noted, however, that fabrics associated with this early thrusting have not been identified in the present study area. Fabrics within the Edgecomb Gneiss and all surrounding stratified rocks are uniformly north to northeast striking and steeply dipping (fig. 4), consistent with later phases of Acadian deformation (see below). Additionally, metamorphic mineral assemblages in all rocks, including the Edgecomb Gneiss (see below), are consistent with Acadian (Devonian) amphibolite facies metamorphism.

Resolving the relative timing relationships between the juxtapositioning of terranes along the Boothbay thrust and the intrusion of the Edgecomb Gneiss protolith magma at *ca.* 413 Ma is critical. In the present study area (fig. 4), the Edgecomb Gneiss is only found within rocks of the Fredericton trough (Bucksport Fm.). Immediately to the south, Hussey and Marvinney (2002) show Edgecomb Gneiss rocks along the contact between the Liberty-Orrington belt (Cape Elizabeth Fm.) and Fredericton trough (Bucksport Fm.), but not cutting across this contact. The

TABLE 2

Whole rock major and trace element geochemical data for representative samples of the Edgecomb Gneiss

(wt. %)	EG-1c	EG-1d	EG-10a	EG-10b	EG-17a	EG-25a	EG-29	EG-43a	EG-43b	EG-49a
SiO_2	61.11	59.81	61.15	62.09	61.76	61.96	59.88	55.81	57.86	57.41
TiO_2	1.12	1.06	1.18	1.06	1.12	0.97	1.07	1.36	1.28	1.31
Al_2O_3	12.50	12.40	12.89	12.75	12.99	12.83	11.82	12.76	13.21	12.21
Fe_2O_3(t)	7.02	6.57	7.12	6.31	6.15	5.74	6.74	8.10	7.72	7.84
MnO	0.12	0.11	0.15	0.13	0.10	0.09	0.11	0.14	0.14	0.13
MgO	7.27	6.94	5.58	6.05	5.74	5.42	7.30	8.11	7.78	7.57
CaO	4.72	4.59	4.44	4.04	4.41	3.92	4.32	5.38	5.40	5.13
Na_2O	2.18	1.10	1.74	1.52	2.51	1.94	1.72	1.54	1.98	1.94
K_2O	3.41	5.84	3.66	4.70	5.13	5.80	5.48	5.06	4.33	4.89
P_2O_5	0.60	0.55	0.60	0.55	0.67	0.47	0.60	0.74	0.67	0.75
Total	100.05	98.97	98.51	99.20	100.58	99.14	99.04	99.00	100.37	99.18
(ppm)										
Sc	19.72	18.91	18.60	18.17	17.04	14.25	17.15	21.81	21.04	22.47
V	149.39	158.45	157.91	140.88	145.65	120.01	134.02	182.97	164.49	182.36
Cr	393.37	411.54	356.50	314.66	264.12	269.32	405.97	433.56	404.78	394.89
Co	27.96	29.33	27.64	24.41	22.81	21.46	27.51	33.86	30.24	30.32
Ni	158.39	162.94	193.83	126.65	103.58	109.25	161.68	167.76	159.50	150.83
Cu	65.48	64.20	10.43	52.05	39.28	41.69	38.33	56.26	19.82	72.18
Zn	107.74	137.66	120.65	160.34	125.57	129.46	128.53	115.17	109.04	132.38
Rb	218.08	245.25	238.02	235.52	201.84	224.51	244.48	216.95	183.66	203.13
Sr	402.80	500.10	368.87	428.56	546.94	530.57	460.40	579.08	536.88	409.61
Y	83.64	25.75	29.29	26.75	25.35	22.43	27.90	28.70	28.72	32.25
Zr	316.63	414.16	448.33	412.54	342.32	328.91	263.69	239.58	288.04	194.95
Nb	23.19	24.15	27.25	22.76	20.37	23.20	23.46	20.68	18.12	22.73
Ba	1229.0	1481.5	1107.3	1882.6	1290.8	1339.1	1336.9	1500.9	1795.2	1311.2
La	57.20	50.04	67.77	59.83	60.22	60.10	49.72	55.21	53.41	75.04
Ce	127.73	113.28	147.17	158.94	132.18	127.11	121.98	128.42	124.73	158.44
Pr	14.97	13.55	18.64	16.30	15.79	14.83	13.14	15.76	15.44	19.38
Nd	59.81	54.80	74.41	65.51	63.97	56.63	54.16	65.54	64.15	78.80
Sm	11.02	10.22	13.23	11.59	11.28	9.93	10.56	12.28	12.22	14.28
Eu	2.00	2.10	2.09	2.14	2.21	1.85	2.03	2.52	2.52	2.56
Gd	7.87	7.39	9.02	8.13	7.97	6.68	7.35	8.99	8.66	10.12
Tb	0.98	0.90	1.10	1.01	0.92	0.80	0.90	1.11	1.04	1.19
Dy	5.77	5.41	6.28	5.65	5.26	4.64	5.42	6.23	5.77	6.83
Ho	1.04	0.97	1.11	0.98	0.92	0.82	0.94	1.11	1.03	1.18
Er	2.75	2.63	3.06	2.74	2.49	2.23	2.58	3.01	2.81	3.20
Tm	0.39	0.36	0.42	0.37	0.33	0.31	0.35	0.41	0.38	0.41
Yb	2.45	2.24	2.77	2.36	2.19	1.96	2.30	2.59	2.47	2.71
Lu	0.38	0.33	0.41	0.34	0.31	0.28	0.33	0.38	0.35	0.38
Hf	8.64	11.08	11.89	11.26	9.13	8.95	7.98	6.65	7.62	5.66
Ta	2.82	2.37	2.85	2.40	1.84	2.40	2.50	1.78	1.83	1.89
Th	37.96	34.82	40.21	35.63	31.31	47.15	40.09	14.24	16.18	37.12
U	5.22	6.24	4.91	6.04	4.09	6.65	6.93	2.50	2.67	3.90

overprinting of the Edgecomb igneous protolith rocks by later Devonian ductile deformation and metamorphism further complicates interpretations of the contact relationships. Frustratingly, these ambiguous field relationships result in uncertainty as to whether the *ca.* 413 Ma Edgecomb Gneiss protolith intrusion pre-dates, or post-dates, terrane juxtapositioning (that is, Boothbay thrust faulting).

In the Discussion section to follow, we assert a correlation between ultrapotassic rocks of the 418 ± 1 Ma Lincoln syenite (fig. 2) and geochemically similar rocks of

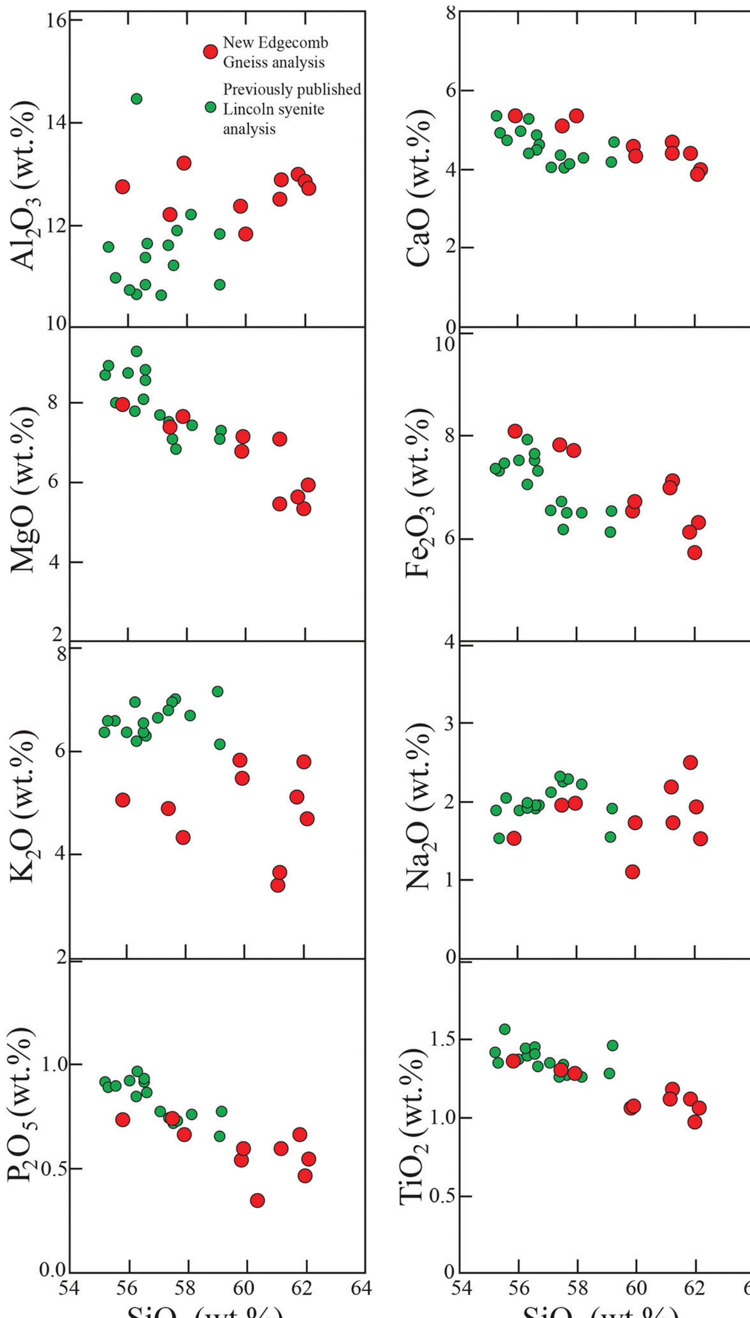

Fig. 8. Harker variation diagrams for major elements in selected samples of the Edgecomb Gneiss (red circles). For comparative purposes (see text), similar data from the Lincoln syenite are plotted in smaller green circles. The Lincoln syenite data are from West and others (2007).

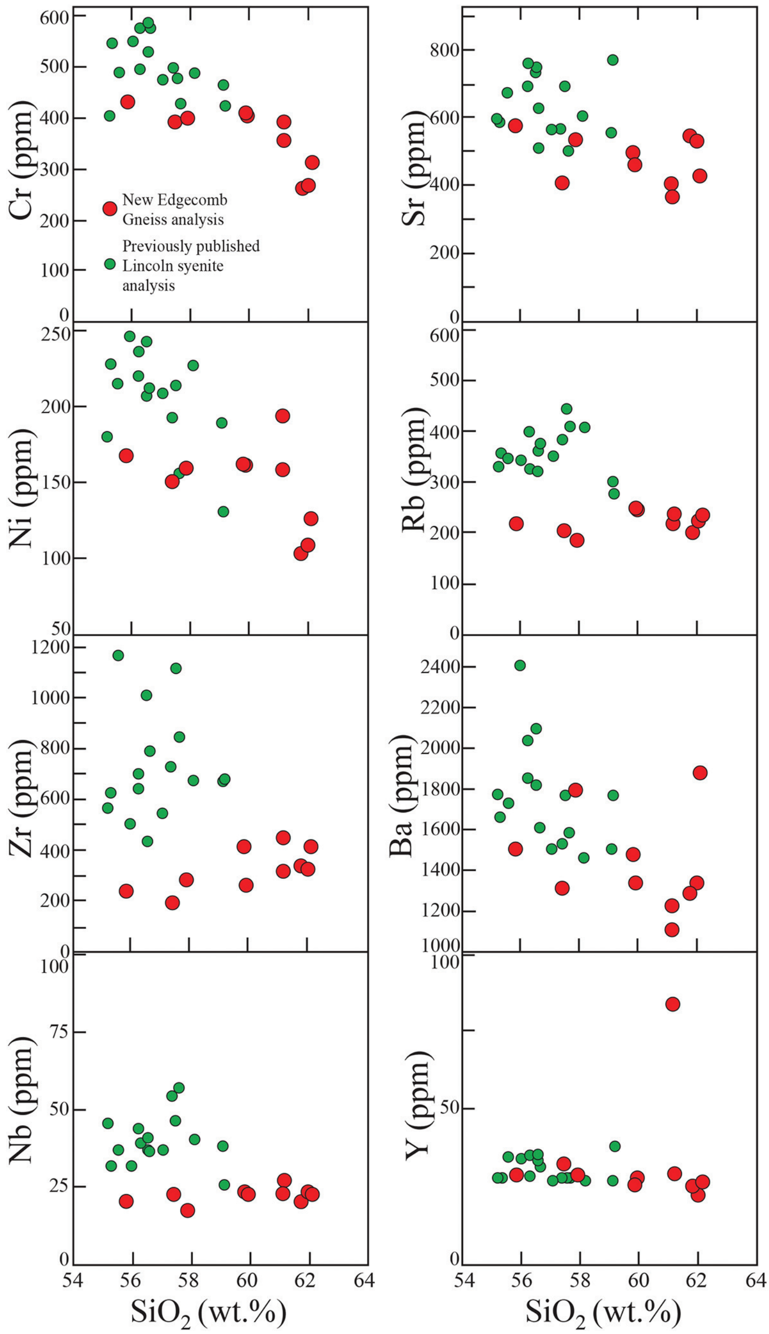

Fig. 9. Harker variation diagrams for selected trace elements in samples of the Edgecomb Gneiss (red circles). For comparative purposes (see text), similar data from the Lincoln syenite are plotted in smaller green circles. The Lincoln syenite data are from West and others (2007).

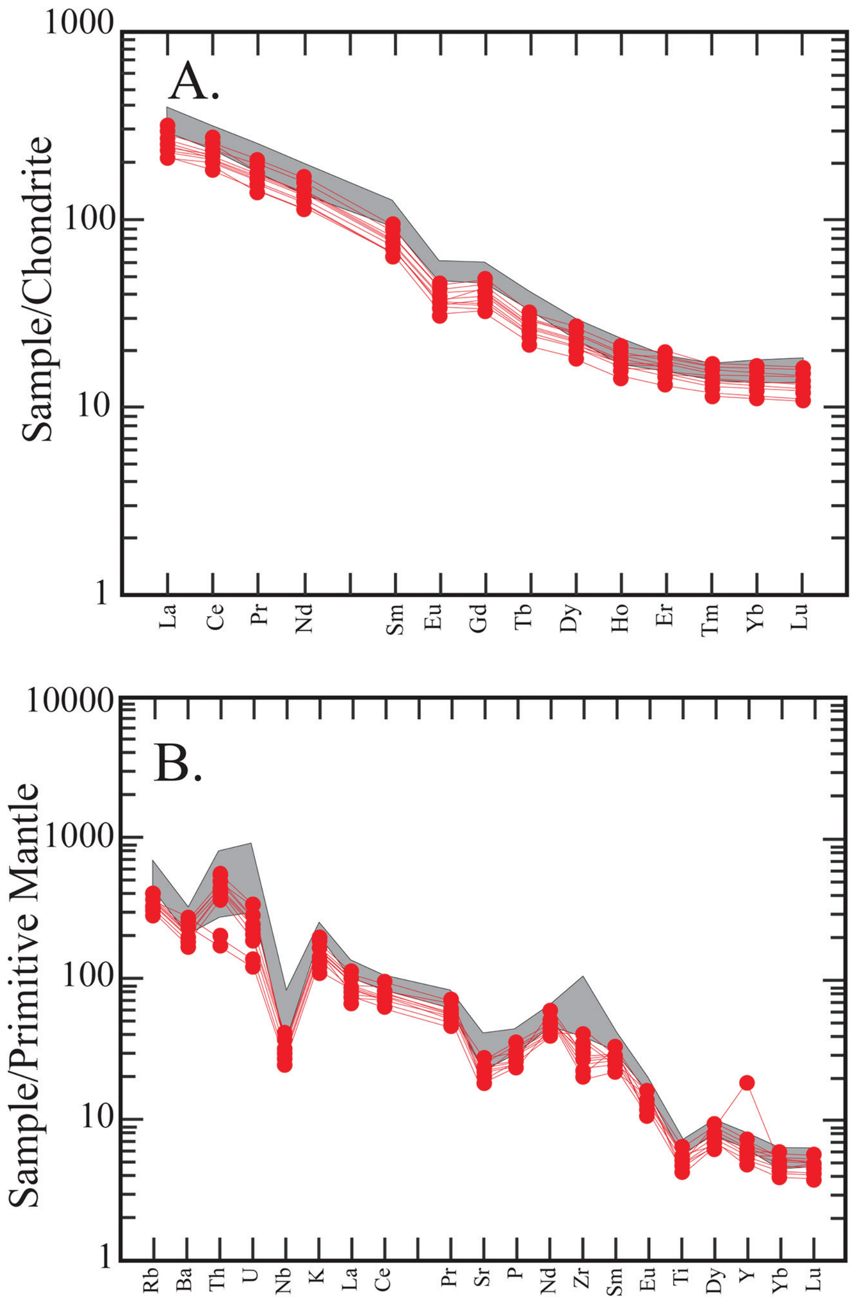

Fig. 10. (A) Chondrite-normalized rare-earth element (REE) data for samples of the Edgecomb Gneiss. (B) Primitive mantle-normalized extended element diagram for rocks of the Edgecomb Gneiss. In both diagrams, the normalizing values are from Sun and McDonough (1989). In both diagrams, for comparative purposes (see text), the range of values from the Lincoln syenite are shown in the gray shaded areas (data from West and others, 2007). Note that Pb, commonly shown on this diagram between Ce and Pr, is not plotted as Pb data was not available from the Lincoln syenite.

the *ca.* 413 Ma Edgecomb Gneiss (figs. 8–10). The Lincoln syenite clearly intrudes rocks of the Liberty-Orrington belt ~40 kilometers to the north (West and others, 2003). Additionally, Hussey and Berry (2002, p. 22–23) in reference to the relationships between sills of the Lincoln syenite to the south of our study area state: "From distribution of the outcrops of the sill, Cape Elizabeth Formation, and the Bucksport Formation, it would appear that the sill cuts across minor folds of the contact and is locally in contact with the two formations implying it postdates the inferred Boothbay thrust." Early Devonian ultrapotassic magmatic rocks are clearly found within both the Liberty-Orrington belt and the Fredericton trough, suggesting close proximity at the time of this geochemically unique magma emplacement. Thus, evidence indicates the initial juxtapositioning of the Casco Bay and Fredericton rocks along the Boothbay thrust pre-dates the intrusion of the 418 ± 1 Ma Lincoln syenite, and by association the ca. 413 Ma Edgecomb Gneiss protolith magma.

Upright folding and associated steep foliation (D_2 deformation).—The most pervasive phase of deformation in the region is characterized by shallow plunging, north to northeast trending, tight to isoclinal, upright folds. These folds are superimposed on all map units, including the Edgecomb Gneiss (fig. 5B), and they deform the Boothbay thrust in multiple places along its length (see the cross-section in fig. 4). Associated with the upright folds is a steeply dipping axial planar foliation that is parallel to compositional layering (transposed?) and pervasive throughout the region. The folds and associated fabrics are correlated with the regionally extensive F_2 folding event of Hussey (1988) in the Casco Bay region, the F_2 folding event of Osberg (1988) in south-central Maine, and more locally the D_3 event of Eusden and others (2016) in the Small Point area. Given that structures associated with this event are found in the nearby 424 ± 2 Ma Blinn Hill granodiorite (see fig. 2 for location, and Tucker and others, 2001 for the radiometric age), and the ca. 413 Ma Edgecomb Gneiss protolith intrusion, this deformational event post-dates these intrusions and marks the main phase of Acadian deformation in the region.

Ductile dextral shear deformation (D_3 deformation).—Superimposed on structures associated with the D_2 deformational event are a wide variety of structures consistent with dextral shear. These include small-scale structures such as asymmetric folds, asymmetric boudinage, shear-band fabrics, as well as thin zones of mylonitic deformation. Within the area of figure 4, the most focused dextral shear can be found along the southeastern margin of the Cape Elizabeth Formation near its contacts with adjacent rocks of the Passagassawakeag Gneiss; these contacts are interpreted to be dextral strike-slip shear zones. This deformational episode is correlated with a prolonged duration of regional dextral transpression that is regionally referred to as the Norumbega Fault and Shear Zone System (Swanson, 1999, 2016).

Brittle faulting (D4 deformation).—The last phase of significant deformation in the area of figure 4 is a late brittle fault, the Back River fault, and associated localized features such as silicified zones and retrograde metamorphism. This fault, first recognized by Hatheway (ms, 1969, referred to as the Edgecomb fault), is located beneath the Sheepscot River estuary and can be traced an additional 15 kilometers to the southeast (Hussey and Marvinney, 2002; West and Hussey, 2020). The Back River fault is easily delineated on geologic maps on the basis of apparent left separation of formational contacts of up to 1.5 kilometers (Hussey, 1992; West, 2016). Although the main trace of this fault is beneath the Sheepscot River, exposures of small-scale brittle faults, contorted foliation orientations, silicified zones, and retrograde metamorphism can be found locally along the shores (West, 2016).

METAMORPHIC HISTORY

Petrographic studies summarized by Hussey and Berry (2002, p. 39) show the study area on the high-grade side of a migmatite front that coincides with the position of a sillimanite + K-feldspar isograd in rocks of pelitic composition. Our observations in the study area agree, as prismatic sillimanite + K-feldspar are a part of the stable mineral assemblage in pelitic rocks of the Cape Elizabeth Formation (see fig. 5F). Although no aluminosilicate minerals other than sillimanite have been observed in the field area, andalusite in pelitic rocks to the southwest (for example, Dunn and Lang, 1988; Eusden and others, 2016) and northeast (West and others, 2003) suggest this metamorphism is relatively low pressure (that is, Buchan style). The stable mineral assemblage in calc-silicate rocks of the Bucksport Formation includes diopside and is consistent with the metamorphic conditions responsible for sillimanite in the pelitic rocks (Ferry, 1976).

The mineralogy and textures observed in rocks of the Edgecomb Gneiss are consistent with the incomplete recrystallization of an initially coarse-grained plutonic rock. Large perthitic K-feldspar, and plagioclase feldspar augen up to 3 cm across are elongated in the plane of foliation (fig. 5A) and commonly mantled by fine-grained neo-crystallized quartz and plagioclase (fig. 5D). These larger grains are separated from one another by strongly foliated domains rich in biotite, actinolite, titanite, and elongated lenses of fine-grained K-feldspar, quartz, and plagioclase. Foliation in these domains is parallel to the pervasive steeply dipping, north-south striking foliation in the surrounding stratified rocks and the axial surfaces of F_2 minor folds. Anhedral clinopyroxene is commonly preserved in the cores of larger calcic amphibole grains (fig. 5C). All of these features are remarkably similar to those present along the sheared margin of the Lincoln syenite in south-central Maine (Marsh and others, 2009).

We found no obvious mineralogical or textural evidence for polymetamorphism in the field area. However, it should be noted this contrasts with the findings of Eusden and others (2016) approximately 30 kilometers to the southwest (Small Point area, see fig. 2) where there is clear evidence of two amphibolite facies metamorphic events recorded in pelitic rocks of the Cape Elizabeth Formation (for example, andalusite + staurolite assemblages/pseudomorphs overprinted by sillimanite-bearing assemblages). However, because metamorphic grade in the present study area is significantly higher, we speculate that if multiple metamorphic events did affect these rocks, the latest event may have obscured evidence of earlier events. Regardless, a $^{40}Ar/^{39}Ar$ hornblende age of 361 ± 4 Ma from just south of the study area indicates the time of cooling following the latest amphibolite facies metamorphic event (West and others, 1993).

DISCUSSION

Field, geochemical, and isotopic data collected along the boundary between Ordovician peri-Gondwanan rocks of the Liberty-Orrington belt and Silurian turbidites of the Fredericton trough are now combined with the results of previous work to provide an integrative tectonic model for the Late Ordovician through Middle Devonian history of this portion of the northern Appalachians. This history is characterized by alternating periods of extension and compression that were likely controlled by temporal changes in subduction dynamics (that is, "tectonic switching" of Collins, 2002). We set the stage by discussing the tectonic origins of the respective terranes in the context of larger scale tectonic processes and follow this with a discussion of how the boundary between these two terranes evolved in time and space during successive tectonic episodes. Figure 11 provides a composite interpretive model for the mid-Paleozoic geodynamic evolution of mid-coastal Maine. We begin at *ca.* 465

Ma with a Laurentian margin including previously accreted rocks of the Moretown terrane (see Karabinos and others, 2017).

Late Ordovician-Early Silurian Liberty-Orrington Belt and Fredericton Trough Tectonic Settings

The Liberty-Orrington terrane of southern Maine is a nearly 175-kilometer long belt that contains Ordovician rocks of the Falmouth-Brunswick and Casco Bay Groups (fig. 1). Previous geochemical (West and others, 2004) and geochronological work (Hussey and others, 2010) have established a correlation with similarly aged rocks in the Miramichi belt of New Brunswick (van Staal and others, 2003) and adjacent Maine (Ludman, 2020). Following the models of van Staal and others (2009, 2016), these rocks are associated with an evolving volcanic arc (Popelogan) to backarc basin (Tetagouche-Exploits) that formed offshore of the Laurentian margin in Middle to Late Ordovician time (fig. 11A). The backarc stage of this tectonic setting is associated with upper-plate extension related to southeast-dipping (present day coordinates) subduction beneath a converging peri-Gondwanan continental crustal fragment (that is, Ganderia). In the present study area, these rocks are represented by feldspathic metasedimentary rocks of the Ordovician Cape Elizabeth Formation. A prominent peak of 600 Ma detrital zircon ages indicate the protolith sediments of these rocks were likely derived from detritus eroding from the Gander crust (Cartwright and others, 2019).

Metasedimentary rocks of the Bucksport Formation in the present study area represent a southern extension of the Fredericton trough and thus are correlated with the Silurian Kingsclear Group in southwestern New Brunswick (Fyffe and others, 2011). The stratigraphy of the Kingsclear Group in the lower grade portions of the belt near the Maine-New Brunswick border has recently been reviewed (Fyffe and others, 2011; Dokken and others, 2018; Ludman and others, 2018) and the Bucksport Formation is likely correlative with the Flume Ridge Formation. Although the belt narrows to less than 10 kilometers wide in south-central Maine (fig. 2), it continues into southern New England as the Merrimack belt (Wintsch and others, 2007). Tectonic models that account for the development of the Silurian Fredericton-Merrimack sedimentary basin have converged on deposition in a syn-accretionary foredeep associated with closure of the aforementioned Tetagouche-Exploits backarc basin (Wilson and others, 2015; Dokken and others, 2018; Ludman and others, 2018, 2020). Closure of the Tetagouche-Exploits backarc basin marks the accretion of all remaining components of the Gander peri-Gondwanan microcontinent with the Laurentian continental margin at this latitude and was accomplished via west-facing subduction beneath Laurentia (van Staal and Barr, 2012; Waldron and others, 2019; and illustrated in fig. 11B).

Late Silurian Terrane Juxtaposition and the Salinic Orogeny

Ordovician rocks of the Liberty-Orrington belt and Silurian rocks of the Fredericton trough are juxtaposed in the study area along the Boothbay thrust (figs. 1 and 2). Along strike to the northeast (figs. 1 and 2) the Boothbay thrust correlates with the Liberty-Orrington thrust of Tucker and others (2001). Further northeast, approximately 120 kilometers from the present study area (fig. 1), the Ordovician Liberty-Orrington belt terminates against Silurian metasedimentary strata of the Fredericton and Central Maine belts (Osberg and others, 1985). Liberty-Orrington belt correlative peri-Gondwanan arc/backarc rocks of Ordovician age reappear to the northeast in the Miramichi belt of eastern Maine and New Brunswick (fig. 1). The equivalent Boothbay/Liberty-Orrington thrust contact in this area, between the western margin of the Fredericton trough and eastern margin of Ordovician peri-Gondwanan arc/backarc rocks (Miramichi belt), lies along the Bamford Brook – Haynesville fault (Fyffe and others, 2011). Pollock and others (2007) and Reusch and van Staal (2012) have suggested that all of these structures correlate with the Dog Bay Line in Newfoundland

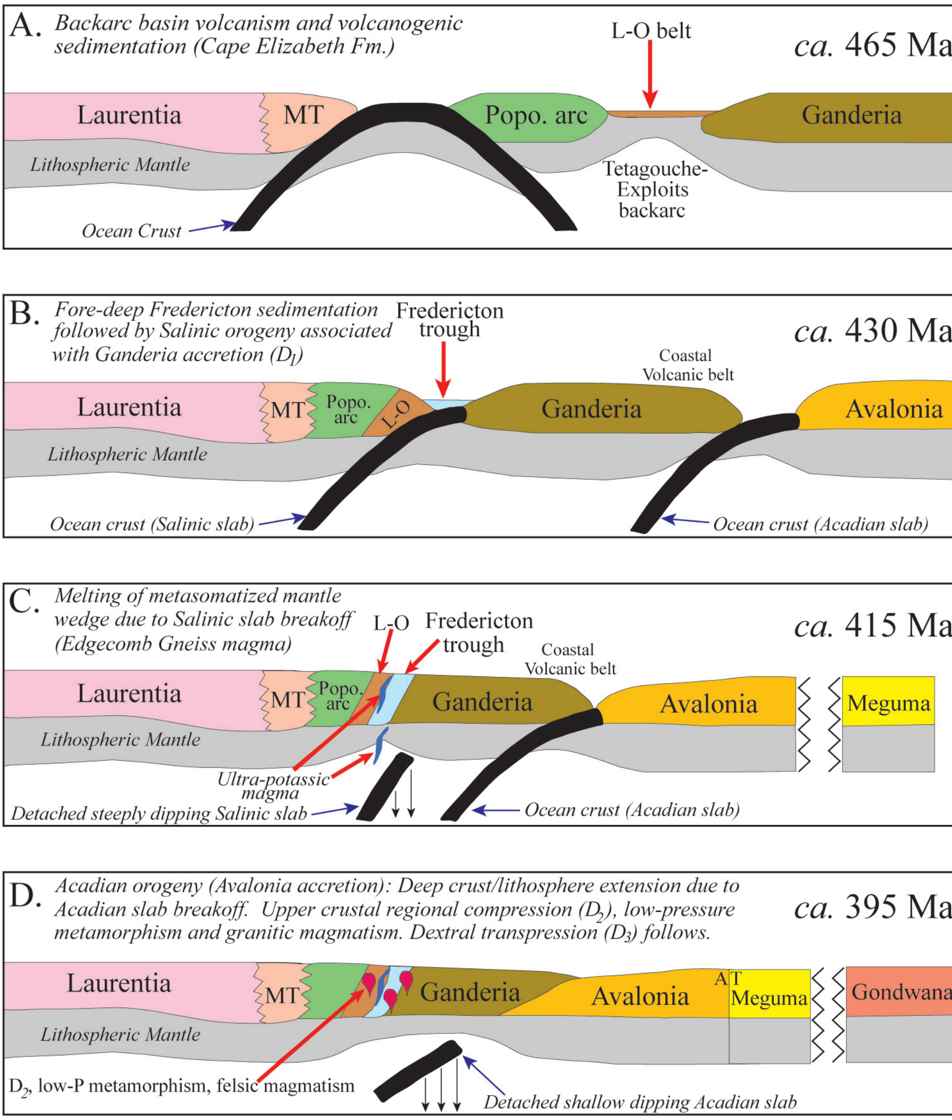

Fig. 11. Schematic cross sections showing the tectonic evolution of the coastal Maine portion of the northern Appalachians from Late Ordovician to Middle Devonian time. Red arrows refer to regions relevant to the study site location. MT = previously accreted Gondwanan-derived Moretown terrane of Macdonald and others (2014); Popo. arc = Early to Middle Ordovician Popelogan volcanic arc of van Staal and others (2016); L-O = Liberty Orrington belt: T = towards and A = away in a regional dextral transpressive setting. Note, for clarity in panels B-D, rocks of the Late Ordovician-Early Devonian Central Maine Basin that cover rocks of the Popelogan arc at the latitude of this study are not shown. Notes on individual panels: (A) The regional model is based on van Staal and others (2009) and van Staal and Barr (2012). The local tectonic setting of the Liberty-Orrington (L-O) belt is based on West and others (2004) and Hussey and others (2010). (B) The regional model is based on Reusch and van Staal (2012), Wilson and others (2015), and Dokken and others (2018). (C) The regional model is based on van Staal and Barr (2012), Llamas and Hepburn (2013), and Wilson and others (2017). The local tectonic setting for the ultra-potassic magmatism is from West and others (2007). (D) The regional scale model is based on van Staal and Barr (2012).

(Williams and others, 1993) and thus collectively they represent a nearly 1000-kilometer long suture marking the final closure of the Iapetus Ocean in the northern Appalachians. It should be noted that in southern New Brunswick, Dokken and others (2018) have suggested this suture lies within the Fredericton trough (Fredericton fault) rather than along its northwestern boundary. At many places along its length, the suture has been modified by overprinting deformation and metamorphism.

The Salinic orogeny marks the closure of the Tetagouche-Exploits backarc basin which had the combined effect of ending sedimentation in the Fredericton trough and juxtaposing the Ordovician peri-Gondwanan arc/backarc rocks of the Liberty-Orrington and Miramichi belts with those of the Fredericton trough along the aforementioned faults. In Maine, previous studies along the Boothbay (Hussey and Berry, 2002, p. 34) and Liberty-Orrington (Tucker and others, 2001, p. 224) faults have advocated for east-verging thrusting and our structural model incorporates this interpretation (fig. 4 cross-section). The correlative structures in eastern-most Maine (Ludman and others, 1993; Ludman, 2020) and adjacent New Brunswick (Fyffe and others, 2011) have also been interpreted to be southeast directed thrust faults prior to reactivation by later strike-slip faulting.

In the Boothbay Harbor region approximately 15 kilometers south of our field area (fig. 2), Hussey and Marvinney (2002) employ isoclinal recumbent folding of the Boothbay thrust to account for the complex structural relationships in that area. However, structural evidence of this folding event is lacking in our field area, and the three-dimensional relationships between units can be more easily explained without incorporating isoclinal recumbent folding (fig. 4 cross-section). Our cross-section is consistent with those shown for areas in the Liberty-Orrington belt to the west and southwest (Hussey and Marvinney, 2002; Eusden and others, 2016; Hussey and West, 2018).

The timing of this first phase of deformation (D_1 thrust faulting) has been well-established in other portions of Maine and is corroborated by our work presented here. Specifically, regional deformation and low-grade metamorphism of Kingsclear Group sedimentary rocks of the Fredericton trough near the Maine-New Brunswick border predate intrusion of the 423 ± 3 Ma Pocomoonshine gabbro-diorite (West and others, 1992). The 418 ± 1 Ma Lincoln syenite (Tucker and others, 2001), located proximal to the study area (fig. 2) also cuts earlier structures (West and others, 2003) and intrudes rocks of both the Liberty-Orrington belt and Fredericton trough (Hussey and Berry, 2002). Although the contact relationship between the intrusion of the igneous protolith of the Edgecomb Gneiss at 412.6 ± 6.0 Ma and the Boothbay thrust is ambiguous (see discussion in the "Deformational History" section), its younger age relative to other cross-cutting intrusive rocks indicates it also must have post-dated the early thrusting. Thus, all available geochronological data from cross cutting plutonic rocks along the length of the Fredericton trough in Maine are consistent with initial juxtapositioning with the Liberty-Orrington belt and the accretion of all remaining components of the Ganderia microcontinent with Laurentia prior to 423 ± 3 Ma. This is consistent with previously published findings in the Canadian Appalachians (for example, stated as being *ca.* 430 Ma, in Wilson and others, 2017) and regional-scale compilations across Maine (Bradley and others, 2000).

Early Devonian Ultra-Potassic Magmatism

The petrologic and geochemical data presented in this paper indicate that the Edgecomb Gneiss protolith was an intrusive igneous rock of intermediate composition. The whole rock geochemistry (figs. 8–10) shows these rocks are ultrapotassic and relatively primitive as inferred from its elevated MgO, Cr, and Ni concentrations. Additionally, the rocks exhibit large ion lithophile element (for example, Ba, Rb, Sr) enrichment relative to high field strength elements (for example, Nb) along with elevated abundances of light rare earth elements (200-300x chondritic abundances).

The ultra-potassic signature of the Edgecomb Gneiss, in combination with the abundance of both crustal-derived large ion lithophile elements and mantle-derived primitive elements, is not common in igneous rocks. However, as shown in figures 8–10, it is similar to the geochemical characteristics of the nearby Lincoln syenite (West and others, 2007), despite the broader spread in SiO_2 concentrations. The ages of these two intrusions overlap within the range of analytical uncertainties (Lincoln syenite = 418 ± 1 Ma, Tucker and others, 2001; Edgecomb Gneiss = 413 ± 6 Ma, this paper). Moreover, approximately 140 kilometers along strike to the northeast (fig. 1), Wang and others (2014) have shown that the Turner Mountain syenite (intrusive age = 410.5 ± 2.5 Ma) shares the unique geochemical signature of the Edgecomb Gneiss and Lincoln Syenite.

These geochemically distinctive ultra-potassic intrusive rocks are restricted in both time (~410–420 Ma) and space (northwestern margin of the Fredericton trough) in the northern Appalachians and suggest a unique petrologic/tectonic setting for their generation. Based on comparisons with rocks of similar composition in known tectonic environments around the world, West and others (2007) proposed a model whereby these ultra-potassic magmas formed as a result of lithospheric extension superimposed on a lithospheric mantle source region previously modified by subduction-driven metasomatism. Wang and others (2014) adopted this model to explain the petrogenesis of the ultra-potassic Turner Mountain syenite in eastern Maine and we similarly adopt the model for the generation of the Edgecomb Gneiss protolith magma.

In addition to the Late Silurian-Early Devonian ultra-potassic magmatism, igneous rocks in coastal Maine with ages between 425 and 410 Ma exist with a much wider range of compositions. Llamas and Hepburn (2013) have argued much of this magmatism formed during west-dipping subduction beneath the eastern margin of Ganderia (illustrated in fig. 11C) and suggest that the wide compositional range in Late Silurian magmatism reflects a transition from continental margin calc-alkaline arc magmatism to bi-modal within plate magmatism associated with the initial stages of Avalonia accretion to the composite Laurentia/Ganderia continental margin. Additionally, Kuiper (2016) has suggested this varied magmatism may have been tied to the progressive subduction of an oceanic ridge in Late Silurian to Early Devonian time. Regardless as to the details of this Acadian subduction-related magmatism (labeled "Coastal Volcanic belt" in figs. 11B and 11C), it was largely outboard (east) of our study area. We propose that the restricted 420 to 410 Ma ultra-potassic magmatism was generated well to the west of the Coastal Volcanic belt due to extension associated with the breakoff of the remnant Salinic oceanic slab (fig. 11C). Decompression melting would have been focused in a deeper region of the lithosphere that had been previously modified by subduction related metasomatism, either during subduction associated with the Ordovician Popelogan arc magmatism (fig. 11A), and/or during Early Silurian Salinic subduction (fig. 11B). Moreover, we suggest the spatially restricted nature of the ultra-potassic magmatism may have been due to a relatively steeply plunging detached Salinic oceanic slab which would have focused magma generating extension (fig. 11C).

Early to Middle Devonian Acadian Deformation and Metamorphism

Following the intrusion of the Edgecomb Gneiss protolith magma at *ca.* 413 Ma, all rocks in the study area were deformed by regional upright folds and an associated steeply dipping penetrative ductile fabric. This deformation, commonly referred to as the main phase of Acadian deformation (D_2 in this study area), is widespread throughout mid-coastal and southern Maine and exerts a dominant control on the strong northeast-trending structural grain in this portion of the northern Appalachians (figs. 1 and 2). This deformation was accompanied by at least one pulse of regional-scale low-pressure amphibolite facies metamorphism. Whereas the first phase of deformation in the study area (D_1) is ascribed to the accretion of the main mass of the Ganderian microcontinent (fig. 11B), this second phase of deformation is attributed to compression associated with the more outboard accretion of the Avalonian microcontinent (fig. 11C and D). Avalonian rocks, sensu stricto, are nowhere exposed at the surface in Maine but are believed to have been underthrust beneath the previously accreted Ganderian microcontinent (van Staal and Barr, 2012, and shown in fig. 11D).

Previous work reveals that the timing of this deformational/thermal event varies across the region and this may reflect a diachroneity to the propagation of the tectonism, and/or that it was long-lived. Just north of the present study area, Tucker and others (2001) published TIMS U-Pb metamorphic monazite ages of 400 to 385 Ma, and monazite and titanite ages of 389-381 Ma from deformed plutonic rocks. Gerbi and West (2007), based on a wide range of SHRIMP U-Pb monazite ages (420–380 Ma) and a similar wide range of plutonic rock ages suggested that this phase of ductile deformation and metamorphism occurred over a period of nearly 40 m.y. In the present study area, it is clear this deformation and metamorphism post-dated the intrusion of the *ca.* 413 Ma Edgecomb Gneiss protolith magma and pre-dated the 368 ± 2 Ma (Tucker and others, 2001) intrusion of the undeformed Waldoboro intrusive complex (fig. 2). Our 399.3 ± 6.6 Ma zircon rims in the Edgecomb Gneiss (fig. 7) fall within this 45 m.y. time frame and thus we interpret them to have grown during D_2 deformation and low-pressure metamorphism. Additionally, this age is consistent with 400 to 380 Ma U-Pb monazite ages reported from metamorphic rocks approximately 30 kilometers to the southwest (Small Point area shown in fig. 2; Peterman and Eusden, 2018) and approximately 40 kilometers to the northeast (Tucker and others, 2001; Gerbi and West, 2007).

Late Devonian and Younger Dextral Shear Deformation

Previous structural studies in mid-coastal (Swanson, 1999, 2016) and south-central (West and Hubbard, 1997; Short and Johnson, 2006) Maine have documented a transition to a strongly dextral transpressive regime in Middle to Late Devonian time and this appears to have extended well into the Carboniferous (West, 1999). The structures include both widely distributed dextral shear deformational features and more localized dextral high-strain zones (West and Hubbard, 1997; Swanson, 1999). Collectively, these types of features have been included in the regionally extensive, complex, and long-lived Norumbega fault and shear zone system (Ludman and West, 1999; Swanson, 2016). In the study area, a wide variety of dextral deformational features, collectively referred to as D_3, are present and consistently overprint earlier ductile structures. Regional scale studies (for example, van Staal and Barr, 2012; Waldron and others, 2015; Tremblay and Pinet, 2016; Wilson and others, 2017) indicate that kinematics throughout much of the northern Appalachians shifted to dextral oblique during this time interval in association with outboard terrane accretion (for example, Meguma, see fig. 11D).

CONCLUSIONS

A synthesis of detailed mapping, structural geology, meta-igneous whole rock geochemistry and U-Pb geochronology along a portion of the regionally significant tectonic boundary between the Ordovician peri-Gondwanan Liberty-Orrington belt and Silurian syn-orogenic strata of the Fredericton trough (a.k.a. the Dog Bay Line of Williams and others, 1993; Reusch and van Staal, 2012) reveal the following important findings:

(1) Initial juxtapositioning of the terranes was accomplished along the east-verging Boothbay thrust fault. This thrusting (D_1) occurred prior to the intrusion of the 418 ± 1 Ma Lincoln syenite, and by association, the *ca.* 413 Ma igneous protolith of the Edgecomb Gneiss. Based on previously published regional relationships, this deformation is associated with the Salinic orogeny and was a result of the accretion of the Ganderia microcontinent to the Laurentian margin prior to 423 ± 3 Ma.

(2) Petrologic, geochemical, and U-Pb isotopic data presented here indicate that the Edgecomb Gneiss was an intermediate igneous rock of ultra-potassic composition that intruded at *ca.* 413 Ma. The distinctive geochemical characteristics of the Edgecomb Gneiss allow for correlations with rocks of similar composition and age (for example, Lincoln Syenite) that occur along an at least 140-kilometer length of the northwestern margin of the Fredericton trough. Generation of the ultra-potassic magma in Early Devonian time was likely the result of the break-off of the descending Salinic oceanic slab beneath the previously accreted Ganderian microcontinent. The extension superimposed on a localized region of previously metasomatized lithospheric mantle resulted in the unique magma composition.

(3) Earlier structures (D_1) and the *ca.* 413 Ma Edgecomb Gneiss igneous protolith were overprinted by upright folding (D_2) and low-pressure amphibolite facies metamorphism. Zircon overgrowths dated at *ca.* 399 Ma in the Edgecomb Gneiss are a product of this period of deformation and metamorphism which is attributed to the Acadian accretion of the outboard Avalonian microcontinent.

(4) Structures consistent with dextral shear deformation are superimposed on all features and reflect a period of Middle Devonian-Carboniferous dextral transpression associated with the Norumbega fault and shear zone system.

ACKNOWLEDGMENTS

This paper has benefited greatly from the thorough reviews of Allan Ludman, Doug Reusch, Cees van Staal, and the extensive comments provided by Associate Editor Robert Wintsch. Funding for the field portion of this work was provided by the Maine Geological Survey through the STATEMAP program. Funding for laboratory analysis was provided by Middlebury College, Bowdoin College, and the Blaustein Fund at Stanford University. Will Amidon and Jody Smith at Middlebury College, and Marty Grove and Christie Jilly-Rehak at Stanford University are thanked for analytical assistance. Discussions with Henry Berry and the late Arthur Hussey over many years have helped shape the ideas presented here.

APPENDIX

Cathodoluminescence images of analyzed zircon grains with ellipses showing spot locations. Uncertainties on individual analyses are reported at 1σ. Red ellipses are interpreted as igneous crystallization, and blue ellipses are interpreted as rims. Dashed ellipses were discordant and not considered in calculating ages. To further document zircon textures, we provide several representative images for grains that were not analyzed.

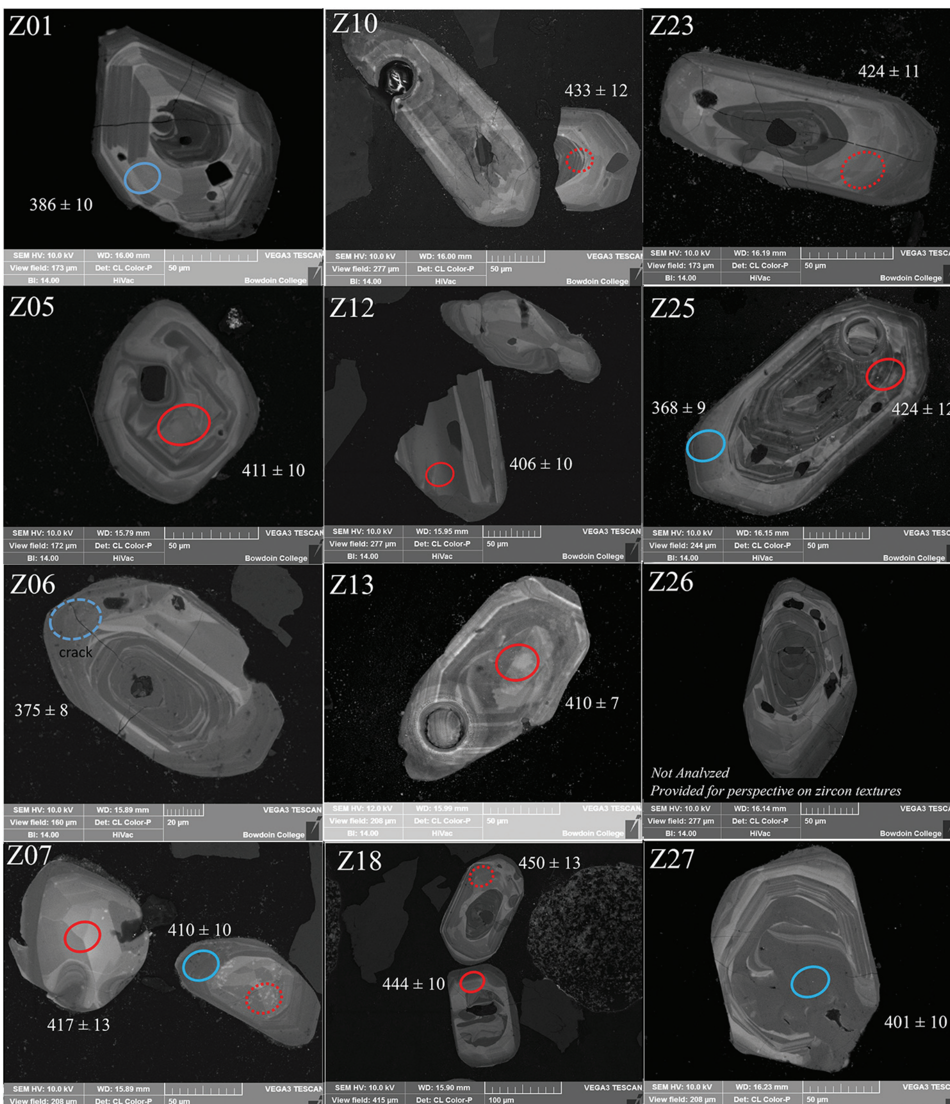

Fig. A1. Samples Z01-Z27.

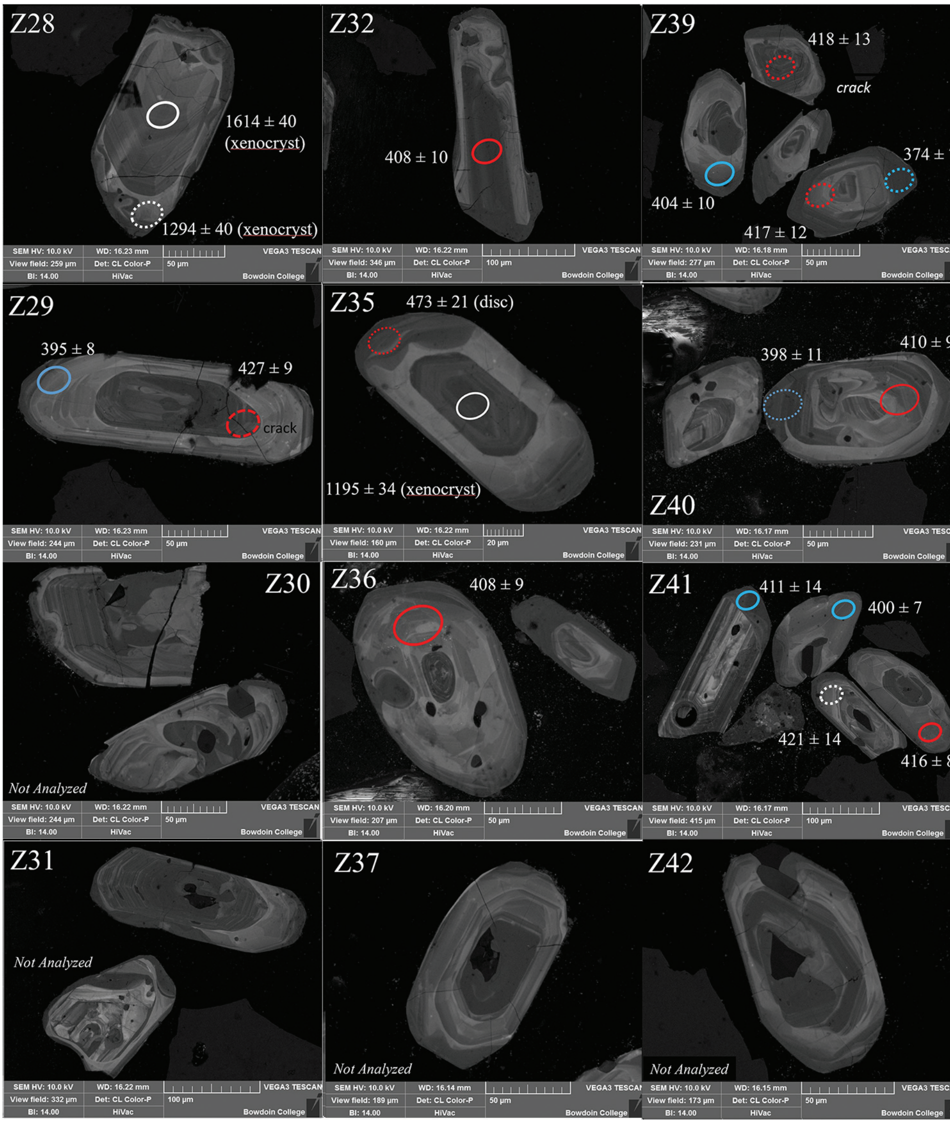

Fig. A1. continued. Samples Z28-Z42.

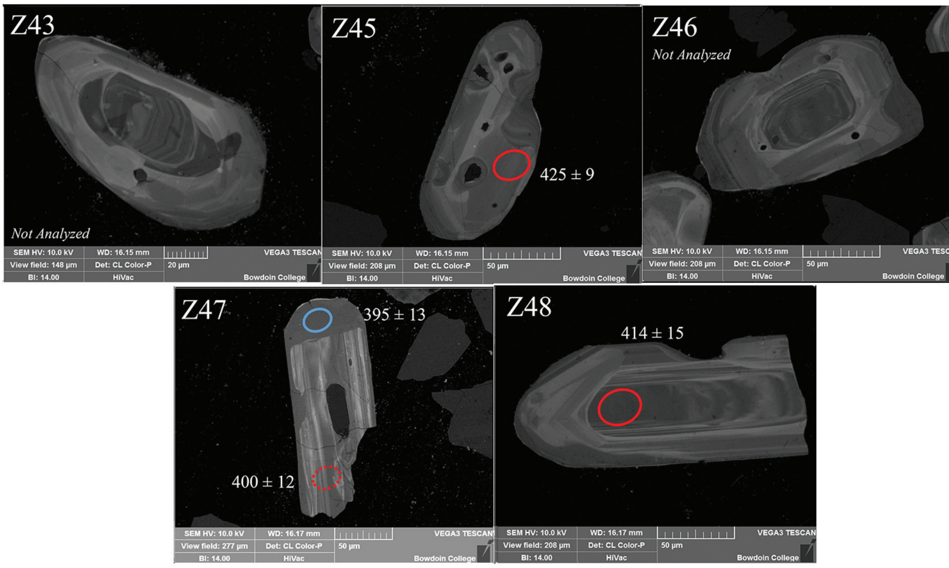

Fig. A1. continued. Samples Z43-Z48.

REFERENCES

Barton, M., and Sidle, W. C., 1994, Petrological and geochemical evidence for granitoid formation: The Waldoboro Pluton Complex, Maine: Journal of Petrology, v. 35, n. 5, p. 1241–1274, https://doi.org/10.1093/petrology/35.5.1241

Berry, H. N., IV, West, D. P., Jr., and Burke, W. B., 2016, Bedrock relationships along the Sennebec Pond fault: A structural puzzle, a stratigraphic enigma, and a tectonic riddle, *in* Berry, H. N., IV and West, D. P., Jr., editors, Guidebook to the Geology of the Maine coast from Maquoit Bay to Muscongus Bay: New England Intercollegiate Geological Conference Guidebook, p. 43–70.

Berry, H. N., IV, and Osberg, P. H., 1989, A stratigraphic synthesis of eastern Maine and western New Brunswick , *in* Tucker, R. D., and Marvinney, R. G., editors, Studies in Maine Geology, Volume 2: Augusta, Maine, Maine Geological Survey, p. 1–29.

Bickel, C. E., 1976, Stratigraphy of the Belfast quadrangle, Maine, *in* Page, L. R., editor, Contributions to the Stratigraphy of New England: Geological Society of America Memoir 148, p. 97–128, https://doi.org/10.1130/MEM148-p97

Black, L. P., Kamo, S. L., Allen, C. M., Aleinikoff, J. N., Davis, D. W., Korsch, R. J., and Foudoulis, C., 2003, TEMORA 1: A new zircon standard for Phanerozoic U-Pb geochronology: Chemical Geology, v. 200, n. 1–2, p. 155–170, https://doi.org/10.1016/S0009-2541(03)00165-7

Bradley, D. C., Tucker, R. D., Lux, D. R., Harris, A. G., and McGregor, D. C., 2000, Migration of the Acadian Orogen and foreland basin across the Northern Appalachians of Maine and adjacent areas: United States Geological Survey Professional Paper 1624, 79 p., https://doi.org/10.3133/pp1624

Cartwright, S. F. A., West, D. P. Jr., and Amidon, W. H., 2019, Depositional constraints from detrital zircon geochronology of strata from multiple lithotectonic belts in south-central Maine, USA: Atlantic Geology, v. 55, p. 93–136, 10.4138/atlg,eol.2019.003

Coble, M. A., Vazquez, J. A., Barth, A. P., Wooden, J., Burns, D., Kylander-Clark, A., Jackson, S., and Vennari, C. E., 2018, Trace element characterization of MAD-559 zircon reference material for ion microprobe analysis: Geostandards and Geoanalytical Research, v. 42, n. 4, p. 481–497, https://doi.org/10.1111/ggr.12238

Collins, W. J., 2002, Hot orogens, tectonic switching, and creation of continental crust: Geology, v. 30, n. 6, p. 535–538, https://doi.org/10.1130/0091-7613(2002)030<0535:HOTSAC>2.0.CO;2

Dokken, R. J., Waldron, J. W. F., and Dufrane, S. A., 2018, Detrital zircon geochronology of the Fredericton trough, New Brunswick, Canada: Constraints on the Silurian closure of remnant Iapetus Ocean: American Journal of Science, v. 318, n. 6, p. 684–725, https://doi.org/10.2475/06.2018.03

Dunn, G. R., and Lang, H. M., 1988, Low pressure metamorphism in the Orrs Island – Harpswell Neck area, Maine: Atlantic Geology, v. 24, n. 3, p. 257–265, https://doi.org/10.4138/1655
Eusden, J. D., Doolittle, H., Grover, T., Lindelof, J., Miller, P., and Sive, H., 2016, Bedrock geology of Small Point, Maine: A fresh look at the stratigraphy, structure, and metamorphism , *in* Berry, H. N., IV, and West, D. P., Jr., editors, Guidebook to the Geology of the Maine coast from Maquoit Bay to Muscongus Bay: New England Intercollegiate Geological Conference Guidebook, p. 129–146.
Ferry, J. M., 1976, Metamorphism of calcareous sediments in the Waterville-Vassalboro area, south-central Maine: Mineral reactions and graphical analysis: American Journal of Science, v. 276, n. 7, p. 841–882, https://doi.org/10.2475/ajs.276.7.841
Foley, S. F., Venturelli, G., Green, D. H., and Toscani, L., 1987, The ultrapotassic rocks: Characteristics, classification, and constraints for petrogenetic models: Earth Science Reviews, v. 24, n. 2, p. 81–134, https://doi.org/10.1016/0012-8252(87)90001-8
Fyffe, L. R., Johnson, S. C., and van Staal, C. R., 2011, A review of Proterozoic to Early Paleozoic lithotectonic terranes in the northeastern Appalachian orogeny of New Brunswick, Canada, and their tectonic evolution during Penobscot, Taconic, Salinic, and Acadian orogenesis: Atlantic Geology, v. 47, p. 211–248, https://doi.org/10.4138/atlgeol.2011.010
Gerbi, C., and West, D. P., Jr., 2007, Use of U-Pb geochronology to identify successive, spatially overlapping tectonic episodes during Silurian-Devonian orogenesis in south-central Maine, USA: GSA Bulletin, v. 119, n. 9–10, p. 1218–1231, https://doi.org/10.1130/B26162.1
Grover, T. W., 2007, Bedrock geology of the North Whitefield 7.5' quadrangle, Maine: Maine Geological Survey Open-File Map 07-57, Scale = 1:24,000.
Grover, T. W., and Newberg, D. W., 2016, Reconnaissance bedrock geology of the Damariscotta 7.5' quadrangle, Maine: Maine Geological Survey Open-File Map 16-22, Scale 1:24,000.
Hatheway, R. B., ms, 1969, Geology of the Wiscasset quadrangle, Maine: Ithaca, New York, Cornell University, Ph. D. thesis, 166 p.
Hibbard, J. P., van Staal, C. R., Rankin, D. W., and Williams, H., 2006, Lithotectonic map of the Appalachian Orogen: Canada-United States of America: Geological Survey of Canada, Map 2096A, scale 1:1,500,000, https://doi.org/10.4095/221932
Hibbard, J. P., van Staal, C. R., and Rankin, D. W., 2007, A comparative analysis of pre-Silurian crustal building blocks of the northern and southern Appalachian orogen: American Journal of Science, v. 307, n. 1, p. 23–45, https://doi.org/10.2475/01.2007.02
Hussey, A. M., II, 1986, Stratigraphic and structural relationships between the Cushing, Cape Elizabeth, Bucksport, and Cross River formations , Portland-Boothbay area, Maine, *in* Newberg, D. W., editor, Guidebook for field trips in southwestern Maine: New England Intercollegiate Geological Conference Guidebook, p. 164–183.
Hussey, A. M., and II, 1988, Lithotectonic stratigraphy, deformation, plutonism, and metamorphism, greater Casco Bay region, southwestern Maine, *in* Tucker, R. D., and Marvinney, R. G., editors, Studies in Maine Geology, Volume 1: Maine Geological Survey, p. 17–34.
——— 1992, The bedrock geology of the Westport 7.5' quadrangle, Maine: Maine Geological Survey Open-File 92-59, 1:24,000 scale map and 9 p. report.
Hussey, A. M., II, and Berry, H. N., IV, 2002, Bedrock Geology of the Bath 1:100,000 map sheet, Coastal Maine: Maine Geological Survey, Bulletin 42, 50 p.
Hussey, A. M., II, and Marvinney, R. G., 2002, Bedrock geology of the Bath 1:100,000 quadrangle, Maine: Maine Geological Survey Map 02-152.
Hussey, A. M., II, and West, D. P., Jr., 2018, Bedrock geology of the Brunswick, 7.5' quadrangle, Maine: Maine Geological Survey Map 18-4, Scale = 1:24,000.
Hussey, A. M., II, Bothner, W. A., and Aleinikoff, J., 2010, The tectono-stratigraphic framework and evolution of southwestern Maine and southeastern New Hampshire, *in* Tollo, R. P., Bartholomew, M. J., Hibbard, J. P., and Karabinos, P.M., editors, From Rodinia to Pangea: The Lithotectonic Record of the Appalachian Region: Geological Society of America Memoir 206, p. 205–230, https://doi.org/10.1130/2010.1206(10)
Karabinos, P., Macdonald, F. A., and Crowley, J. L., 2017, Bridging the gap between the foreland and hinterland I: Geochronology and plate tectonic geometry of Ordovician magmatism and terrane accretion on the Laurentian margin of New England: American Journal of Science, v. 317, n. 5, p. 515–554, https://doi.org/10.2475/05.2017.01
Kuiper, Y. D., 2016, Development of the Norumbega fault system in mid-Paleozoic New England, USA: An integrated subducted oceanic ridge model: Geology, v. 44, n. 6, p. 455–458, https://doi.org/10.1130/G37599.1
Llamas, A. P., and Hepburn, J. C., 2013, Geochemistry of Silurian-Devonian volcanic rocks in the Coastal Volcanic belt, Machias-Eastport area, Maine: Evidence for a pre-Acadian arc: GSA Bulletin, v. 125, n. 11–12, p. 1930–1942, https://doi.org/10.1130/B30776.1
Ludman, A., 2020, Bedrock geology of the Greenfield quadrangle, Maine: Maine Geological Survey Open-File Report 20-10, 1:24,000 map scale and 28 p. report.
Ludman, A., and West, D. P., Jr., editors, 1999, Norumbega Fault System of the Northern Appalachians: Geological Society of America Special Paper 331, 199 p., https://doi.org/10.1130/SPE331
Ludman, A., Hopeck, J. T., and Brock, P. C., 1993, Nature of the Acadian orogeny in eastern Maine, *in* Roy, D. C., and Skehan, J. W., editors, The Acadian Orogeny: Recent Studies in New England, Maritime Canada, and the Autochthonous Foreland: Geological Society of America Special Paper 275, p. 67–84, https://doi.org/10.1130/SPE275-p67
Ludman, A., Aleinikoff, J., Berry, H. N., IV, and Hopeck, J. T., 2018, SHRIMP U-Pb zircon evidence for age, provenance, and tectonic history of early Paleozoic Ganderian rocks, east-central Maine, USA: Atlantic Geology, v. 54, p. 335–387, https://doi.org/10.4138/atlgeol.2018.012

Ludman, A., Machado, G., and Fernandes, P., 2020, Palynological dating of low-grade metamorphosed rocks: Applications to Early Paleozoic rocks of the Central Maine/Aroostook-Matapedia Basin and Fredericton trough (northern Appalachians) in eastern and east-central Maine, U.S.A., American Journal of Science, v. 320, n. 3, p. 280–312, https://doi.org/10.2475/03.2020.03

Ludwig, K. R., 2009, Squid 2, A user's manual: Berkeley, California, Berkeley Geochronology Center Special Publication 5, 110 p.

——— 2012, User's Manual for Isoplot Version 3.75–4.15: A Geochronological Toolkit for Microsoft Excel: Berkeley, California, Berkeley Geochronological Center Special Publication 5.

Macdonald, F. A., Ryan-Davis, J., Coish, R. A., Crowley, J. L., and Karabinos, P., 2014, A newly identified Gondwanan terrane in the northern Appalachian Mountains: Implications for the Taconic orogeny and closure of the Iapetus Ocean: Geology, v. 42, n. 6, p. 539–542, https://doi.org/10.1130/G35659.1

Marsh, J. H., Johnson, S. E., Yates, M. G., and West, D. P., Jr., 2009, Coupling of deformation and reactions during mid-crustal shear zone development: An *in situ* frictional-viscous transition: Journal of Metamorphic Geology, v. 27, n. 8, p. 531–553, https://doi.org/10.1111/j.1525-1314.2009.00841.x

Mattinson, J. M., 2010, Analysis of the relative decay constants of ^{235}U and ^{238}U by multi-step CA-TIMS measurements of closed-system natural zircon samples: Chemical Geology, v. 275, n. 3–4, p. 186–198, https://doi.org/10.1016/j.chemgeo.2010.05.007

McKerrow, W. S., and Ziegler, A. M., 1971, The lower Silurian paleogeography of New Brunswick and adjacent areas: The Journal of Geology, v. 79, n. 6, p. 635–646, https://doi.org/10.1086/627695

Osberg, P. H., 1988, Geologic relations within the shale-wacke sequence in south-central Maine, *in* Tucker, R. D., and Marvinney, R. G., editors, Studies in Maine Geology, Volume 1, Structure and Stratigraphy: Maine Geological Survey Publications 54, p. 51–74.

Osberg, P. H., and Berry, H. N., IV, 2020, Bedrock geology of the Camden quadrangle, Maine: Maine Geological Survey Open-File Map 20-8, Scale 1:24,000.

Osberg, P. H., Hussey, A. M. II, and Boone, G. M., 1985, Bedrock Geologic Map of Maine: Maine Geological Survey, Scale 1:500,000.

Peterman, E. M., and Eusden, J. D., Jr., 2018, Monazite geochronology records early Acadian and Neoacadian tectonometamorphic events in midcoast Maine: Geological Society of America Abstracts with Programs, v. 50, n. 2,10.1130/abs/2018NE-310226

Peterman, E. M., Jercinovic, M. J., Beane, R. J., and de Wet, C. B., 2021, Kyanite preserves prograde and retrograde metamorphic events as revealed by cathodoluminescence, geochemistry and crystallographic orientation. Journal of Metamorphic Geology, https://doi.org/10.1111/jmg.12593

Pollock, J. C., Wilton, D. H. C., van Staal, C. R., and Morrissey, K. D., 2007, U-Pb detrital zircon geochronological constraints on the Early Silurian collision of Ganderia and Laurentia along the Dog Bay Line: The terminal Iapetan suture in the Newfoundland Appalachians: American Journal of Science, v. 307, n. 2, p. 399–433, https://doi.org/10.2475/02.2007.04

Pollock, S. G., 2018, Bedrock geology of the Brooks East quadrangle, Maine: Maine Geological Survey, Open-File Map 18-15, scale 1:24,000.

Reusch, D. N., and van Staal, C. R., 2012, The Dog Bay – Liberty Line and its significance for Silurian tectonics of the northern Appalachian orogen: Canadian Journal of Earth Sciences, v. 49, n. 1, p. 239–258, https://doi.org/10.1139/e11-024

Short, H. A., and Johnson, S. E., 2006, Estimation of vorticity from fibrous calcite veins, central Maine, USA: Journal of Structural Geology, v. 28, n. 7, p. 1167–1182, https://doi.org/10.1016/j.jsg.2006.03.024

Sun, S. S., and McDonough, W. F. 1989, Chemical isotope systematics of the oceanic basalts: Implications for mantle composition and processes, *in* Saunders, A. D., and Norry, M. J., editors, Magmatism in the Ocean Basins: Geological Society, London, Special Publications, v. 42, p. 313–345, https://doi.org/10.1144/GSL.SP.1989.042.01.19

Swanson, M. T., 1999, Dextral transpression at the Casco Bay restraining bend, Norumbega fault zone, coastal Maine, *in* Ludman, A., and West, D. P., Jr., editors, Norumbega Fault System of the Northern Appalachians: Geological Society of America Special Paper 331, p. 85–104, https://doi.org/10.1130/0-8137-2331-0.85

——— 2016, Kinematic indicators and ductile strain domains associated with regional shearing: A transect across the Norumbega fault and shear zone system, Pemaquid Point to northern Casco Bay, *in* Berry, H. N. IV, and West, D. P., Jr., editors, Guidebook to the Geology of the Maine coast from Maquoit Bay to Muscongus Bay: New England Intercollegiate Geological Conference Guidebook, p. 1–18.

Tremblay, A., and Pinet, N., 2016, Late Neoproterozoic to Permian tectonic evolution of the Quebec Appalachians, Canada: Earth Science Reviews, v. 160, p. 131–170, https://doi.org/10.1016/j.earscirev.2016.06.015

Tucker, R. D., Osberg, P. H., and Berry, H. N., IV, 2001, The geology of a part of Acadia and the nature of the Acadian orogeny across central and eastern Maine: American Journal of Science, v. 301, n. 3, p. 205–260, https://doi.org/10.2475/ajs.301.3.205

van Staal, C. R., and Barr, S. M., 2012, Lithospheric architecture and tectonic evolution of the Canadian Appalachians and associated Atlantic margin, *in* Percival, J. A., Cook, F. A., and Clowes, R. M., editors, Tectonic Styles in Canada: The Lithoprobe Perspective: Geological Association of Canada Special Paper 49, Chapter 2, p. 41–95.

Van Staal, C. R., and Williams, P. F., 1988, Collision along an irregular margin: A regional plate tectonic interpretation of the Canadian Appalachians: Discussion: Canadian Journal of Earth Sciences, v, 25, n. 11, p. 1912–1916, https://doi.org/10.1139/e88-180

van Staal, C. R., Wilson, R. A., Rogers, N., Fyffe, L. R., Langton, J. P., McCutcheon, S. R., McNicoll, V., and Ravenhurst, C. E., 2003, Geology and tectonic history of the Bathurst Supergroup, Bathurst Mining Camp, and its relationships to coeval rocks in southwestern New Brunswick and adjacent Maine—A synthesis, *in* Goodfellow, W. D., McCutcheon, S. R., and Peter, J. M., editors, Massive Sulfide Deposits of the Bathurst Mining Camp, New Brunswick, and Northern Maine: Economic Geology Monographs, v. 11, p. 37–60, https://doi.org/10.5382/Mono.11.03

van Staal, C. R., Whalen, J. B., Valverde-Vaquero, P., Zagorevski, A., and Rodgers, N., 2009, Pre-Carboniferous, episodic accretion-related orogenesis along the Laurentian margin of the northern Appalachians, *in*, , Murphy, J. B., Keppie, J. D., and Hynes, A. J., editors, Ancient Orogens and Modern Analogues: Geological Society, London, Special Publications, v. 327, p. 271–316, https://doi.org/10.1144/SP327.13

van Staal, C. R., Wilson, R. A., Kamo, S. L., McClellan, W. C., and McNicoll, V., 2016, Evolution of the Early to Middle Ordovician Popelogan arc in New Brunswick Canada and adjacent Maine, USA: Record of arc-trench migration and multiple phases of rifting: GSA Bulletin, v. 128, n. 1–2, p. 122–146, https://doi.org/10.1130/B31253.1

Waldron, J. W. F., Barr, S. M., Park, A. F., White, C. E., and Hibbard, J., 2015, Late Paleozoic strike-slip faults in Maritime Canada and their role in the reconfiguration of the northern Appalachian orogen: Tectonics, v. 34, n. 8, p. 1661–1684, https://doi.org/10.1002/2015TC003882

Waldron, J. W. F., Schofield, D. I., and Murphy, J. B., 2019, Diachronous Paleozoic accretion of peri-Gondwanan terranes at the Laurentian margin, *in* Wilson, R. W., Housman, G. A., McCaffrey, K. J. W., Doré, A. G., and Buiter, S. J. H., editors, Fifty years of the Wilson Cycle Concept in Plate Tectonics: Geological Society, London, Special Publications, v. 470, p. 289–310, https://doi.org/10.1144/SP470.11

Wang, C., Ludman, A., and Xiao, L., 2014, The Turner Mountain syenite, Maine, USA: geology, geochemistry, geochronology, petrogenesis, and post-orogenic exhumation: Atlantic Geology, v. 50, p. 233–248, https://doi.org/10.4138/atlgeol.2014.012

West, D. P., Jr., 1999, The timing of displacements along the Norumbega fault system, south-central and south-coastal Maine , *in* Ludman, A., and West, D. P., Jr., editors, The Norumbega Fault System of the Northern Appalachians: Geological Society of America Special Paper 331, p. 167–178, https://doi.org/10.1130/0-8137-2331-0.167

——— 2006, Bedrock Geology of the Washington 7.5' Quadrangle, Maine: Maine Geological Survey Map 06-79, Scale 1:24,000.

——— 2016, Bedrock geology of the Wiscasset 7.5' quadrangle, Maine: Maine Geological Survey Open-File Map 16-27, Scale = 1:24,000.

West, D. P., Jr., and Condit, C. B., 2016, Stratigraphy, structure, and plutonism in the Wiscasset-Dresden region of mid-coastal Maine, *in* Berry, H. N. IV, , and West, D. P., Jr., editors, Guidebook to the Geology of the Maine coast from Maquoit Bay to Muscongus Bay: New England Intercollegiate Geological Conference Guidebook, p. 165–182.

West, D. P., Jr., and Hubbard, M. S., 1997, Progressive localization of deformation during exhumation of a major strike-slip shear zone: Norumbega fault zone, south-central Maine, USA: Tectonophysics, v. 273, n. 3–4, p. 185–201, https://doi.org/10.1016/S0040-1951(96)00306-X

West, D. P., Jr., and Hussey, A. M., II, 2020, Bedrock geology of the Bath quadrangle, Maine: Maine Geological Survey Open-File Map 20-12, Scale 1:24,000.

West, D. P. Jr., Ludman, A., and Lux, D. R., 1992, Silurian age for the Pocomoonshine Gabbro-Diorite, southeastern Maine and its regional tectonic implications: American Journal of Science, vol. 292, n. 4, p. 253–273, 10.2475/ajs.292.4.253

West, D. P., Jr., Lux, D. R, and Hussey, A. M., II, 1993, Contrasting thermal histories across the Flying Point fault, southwestern Maine: Evidence for Mesozoic displacement: GSA Bulletin, v. 105, n. 11, p. 1478–1490, https://doi.org/10.1130/0016-7606(1993)105<1478:CTHATF>2.3.CO;2

West, D. P., Jr., Beal, H. M., and Grover, T. W., 2003, Silurian deformation and metamorphism of Ordovician arc rocks of the Casco Bay Group, south-central Maine: Canadian Journal of Earth Sciences, v. 40, p. 887–905, https://doi.org/10.1139/e03-021

West, D. P., Jr., Coish, R. A., and Tomascak, P. B., 2004, Tectonic setting and regional correlation of Ordovician meta-volcanic rocks of the Casco Bay Group, Maine: Evidence from trace element and isotope geochemistry: Geological Magazine, v. 141, n. 2, p. 125–140, https://doi.org/10.1017/S0016756803008562

West, D. P., Jr., Tomascak, P. B., Coish, R. A., Yates, M. G., and Reilly, M. J., 2007, Petrogenesis of the ultra-potassic Lincoln Syenite, Maine: Late Silurian-Early Devonian melting of a source region modified by subduction driven metasomatism: American Journal of Science, v. 307, n. 1, p. 265–310, https://doi.org/10.2475/01.2007.08

Whitney, D. L., and Evans, B. W., 2010, Abbreviations for names of rock-forming minerals: American Mineralogist, v. 95, n. 1, p. 185–187, 10.2138/am.2010.3371

Wilson, R. A., van Staal, C. R., and McClelland, W. C., 2015, Synaccretionary sedimentary and volcanic rocks in the Ordovician Tetagouche backarc basin, New Brunswick, Canada: Evidence for a transition from foredeep to forearc basin sedimentation: American Journal of Science, v. 315, n. 10, p. 958–1001, https://doi.org/10.2475/10.2015.03

Wilson, R. A., van Staal, C. R., and Kamo, S. L., 2017, Rapid transition from the Salinic to Acadian orogenic cycles in the northern Appalachian orogen: Evidence from northern New Brunswick, Canada: American Journal of Science, v. 317, n. 4, p. 449–482, https://doi.org/10.2475/04.2017.02

Wintsch, R. P., Aleinikoff, J. N., Walsh, G., Bothner, W. A., Hussey, A. M., II, and Fanning, C. M., 2007, SHRIMP U-Pb evidence for a Late Silurian age of metasedimentary rocks in the Merrimack and Putnam-Nashoba terranes, eastern New England: American Journal of Science, v. 307, n. 1, p. 119–167, https://doi.org/10.2475/01.2007.05

Williams, H., Currie, K. L., and Piasecki, M. A. J., 1993, The Dog Bay Line: A major Silurian tectonic boundary in northeast Newfoundland: Canadian Journal of Earth Sciences, v. 30, p. 2481–2494, 10.1139/e93-215